Mechanisms of Resistance to New Generation Anti-TB Drugs

by

Hanri Visser

Thesis submitted in partial fulfilment of the requirements for the degree of Master of Science in Molecular Biology at the Faculty of Medicine and Health Sciences, University of Stellenbosch

DST/NRF Centre of Excellence for Biomedical Tuberculosis Research
Division of Molecular Biology and Human Genetics
Faculty of Medicine and Health Sciences
Stellenbosch University
PO Box 19063; Francie van Zijl Drive
Tygerberg 7505
South Africa

Supervisor: Prof. T.C. Victor

Co-Supervisor: Dr L.V. Paul

Faculty of Medicine and Health Sciences

March 2015

Declaration

By submitting this thesis electronically, I declare that the entirety of the work contained therein is my own, original work, that I am the authorship owner thereof (unless to the extent explicitly otherwise stated) and that I have not previously in its entirety or in part submitted it for obtaining any qualification.

Date: November 2014 _____

Summary

Drug resistance in *Mycobacterium tuberculosis* is an increasing global problem. Drug resistance is mostly caused by single nucleotide polymorphisms (SNPs) within the bacterial genome. This observed increase in global incidence of drug resistant tuberculosis (TB) has sparked the search for new anti-TB drugs and the repurposing of drugs that are currently used against other organisms or species of mycobacteria. One such repurposed drug, clofazimine (CFZ), is currently used for the treatment of leprosy, caused by *Mycobacterium leprae*. The mechanism of action of CFZ is not clear, but it is hypothesized that CFZ is reduced by a mycobacterial type II NADH oxidoreductase (NDH-2). The reduction of CFZ drives the production of reactive oxygen species (ROS) which is toxic to the pathogen. The aim of this study was to elucidate the mechanism of CFZ resistance. Towards this aim, spontaneous *in vitro* CFZ resistant mutants were selected, characterized and whole genome was used identify SNPs which may cause CFZ resistance. Mutations were identified in a transcriptional regulator encoded by *Rv0678*, fatty-acid-AMP ligase, or FadD28 (*Rv2941*) and glycerol kinase or GlpK (*Rv3696c*). Mutations in *Rv0678* have previously been shown to play a role in both CFZ resistance and bedaquiline (BDQ) cross-resistance, while no link has been found between CFZ resistance and mutations in *fadD28* and *glpK*. The novel, non-synonymous SNP identified in *Rv0678* resulted in the replacement of an alanine residue with threonine at codon 84, which is located in the DNA binding domain. Virtual modelling of the mutated Rv0678 protein showed that the A84T mutation may influence DNA binding, possibly due to its proximity to the DNA binding domain. This mutation caused a change in hydrophobicity, which may influence binding to DNA. Previous studies showed that mutations in *Rv0678* resulted in the upregulation of *mmpL5*, a putative efflux pump. However, the mechanism whereby CFZ resistance occurs via increased abundance of this efflux pump in the cell wall is not clear and needs further investigation. The cross-resistance between CFZ and BDQ, caused by mutations in *Rv0678*, is of concern and may influence the planning of anti-TB drug regimens for the future. The roles of the other two mutations identified in this study in CFZ resistance is also not clear and requires further investigation. Finally, the findings of this study support the role of *Rv0678* in CFZ resistance thereby suggesting that this gene could be useful as a diagnostic marker to test for CFZ resistance in clinical isolates.

Opsomming

Middelweerstandigheid in *Mycobacterium tuberculosis* is 'n wêreldwye toenemende probleem. Middelweerstandigheid word meestal veroorsaak deur enkel nukleotied polimorfismes (SNPs) in die bakteriële genoom. Hierdie toename in middelweerstandige tuberkulose (TB) het gelei tot die soektog na nuwe anti-TB-middels en die alternatiewe aanwending van middels wat tans teen ander organismes of spesies van mikobakterieë gebruik word. Een so 'n alternatiewe middel, clofazimine (CFZ), word tans gebruik vir die behandeling van melaatsheid wat veroorsaak word deur *Mycobacterium leprae*. CFZ se meganisme van werking is nie duidelik nie, maar dit word vermoed dat CFZ gereduseer word deur 'n mikobakteriële tipe II NADH oksidoreduktase (NDH-2). Die reduksie van CFZ dryf die produksie van reaktiewe suurstof spesies wat giftig is vir die patogeen. Die doel van hierdie studie was om die meganisme van CFZ weerstandigheid te ondersoek. Om hierdie doel te bereik was spontane *in vitro* CFZ weerstandige mutante gekies, gekarakteriseer en heel genoom volgorde bepaling is gebruik om SNPs te identifiseer wat CFZ weerstandigheid veroorsaak. Mutasies in *Rv0678*, 'n transkripsie reguleerder, vetsuur-AMP ligase, of FadD28 (*Rv2941*) en gliserol kinase of GlpK (*Rv3696c*) geïdentifiseer. Dit is al voorheen gevind dat mutasies in *Rv0678* ‘n rol speel in beide CFZ weerstandigheid en bedaquiline (BDQ) kruis-weerstandigheid, terwyl geen verband gevind is tussen CFZ weerstandigheid en mutasies in *fadD28* en *glpK* nie. Die nuwe, nie-sinonieme SNP, geïdentifiseer in *Rv0678* het gelei to die vervanging van 'n alanien aminosuur met treonien by kodon 84, wat geleë is in die DNS bindings domein. Virtuele modellering van die gemuteerde Rv0678 proteïen het getoon dat die A84T mutasie DNS binding moontlik kan beïnvloed, as gevolg van sy nabyheid aan die DNS bindings domein. Hierdie mutasie veroorsaak 'n verandering in die hidrofobiese natuur, wat DNS binding kan beïnvloed. Vorige studies het getoon dat mutasies in *Rv0678* lei tot die opregulering van *mmpL5*, 'n waarskynlike uitvloei pomp. Die meganisme waardeur CFZ weerstandigheid veroorsaak, deur ‘n groot aantal van hierdie uitvloei pompe in die selwand, is nie duidelik nie en moet verder ondersoek word. Die kruis-weerstandigheid tussen CFZ en BDQ, wat veroorsaak word deur mutasies in *Rv0678*, is van belang en kan die beplanning van anti-TB middel behandeling vir die toekoms beïnvloed. Die rolle van die ander twee mutasies, wat in hierdie studie geïdentifiseer is, in CFZ weerstandigheid is ook nie duidelik nie en vereis verdere ondersoek. Ten slotte, die bevindinge van hierdie studie steun die rol van *Rv0678* in CFZ weerstandigheid en dit dui daarop dat hierdie geen gebruik kan word as 'n diagnostiese merker om vir CFZ weerstandigheid te toets in kliniese isolate.

Acknowledgments

I would like to express my sincerest thanks to the following people and institutions that accompanied and helped me through the writing of this thesis.

- My supervisor Prof Tommie Victor, co-supervisor Dr Lynthia Paul, Prof Rob Warren and Prof Samantha Sampson for guidance and many suggestions and discussions during the writing of this thesis.

- My colleagues and friends in the Division of Molecular Biology and Human Genetics, especially everyone in Lab 453.

- Dr Margaretha de Vos and Dr Ruben van der Merwe who helped me understand and apply the bioinformatics used in this thesis.

- The National Research Foundation (NRF), Harry Crossley Foundation and Stellenbosch University for funding.

- All my friends, especially Gideon Engelbrecht, Danielle van Blerk and Henk Botha, for the support and laughs that kept me sane during the writing of this thesis.

- My parents (Dirk Visser, Lenette Visser), brother (Dirkie Visser) and sister (Carla Visser) who enabled me to write this thesis through their love and support.

Table of Content

List of Figures

List of Tables

Abbreviations

7H9+ADC	Middlebrook 7H9 broth + Albumin Dextrose Catalase + 0.5% Tween + 0.2% Glycerol
7H10+OADC	Middlebrook 7H10 agar + Oleic Albumin Dextrose Catalase + 2% Glycerol
7H10+OADC+CFZ	Middlebrook 7H10 agar + Oleic Albumin Dextrose Catalase + 2% Glycerol + Clofazimine
^{o}C	Degree Celsius
µg	Microgram
µl	Microliter
AA	Amino Acid
ADC	Albumin Dextrose Catalase
ADME	Absorption, Distribution, Metabolism and Excretion
AMK	Amikacin
ATP	Adenosine Triphosphate
BDQ	Bedaquiline
bp	Basepairs
CAP	Capreomycin
cDNA	Complementary Deoxyribonucleic Acid
CFZ	Clofazimine
CFU	Colony Forming Unit
CYC	Cycloserine
DMSO	Dimethyl Sulfoxide
DNA	Deoxyribonucleic Acid
DNB	Dinitrobenzamide Derivatives
dNTP	Deoxynucleotide
DOTS	Directly Observed Therapy – Short Course

DprE1	Decaprenylphosphoryl-β-D-Ribose 2'-Epimerase
DST	Drug Susceptibility Test
EBA	Early Bacterial Activity
ECL	Electrochemiluminescent
EDTA	Ethylenediaminetetraacetic Acid
EMB	Ethambutol
ETC	Electron Transport Chain
ETH	Ethionamide
FadD28	Fatty-acid-AMP Ligase
FDA	Food and Drug Administration
GAT	Gatifloxacin
GATK	Genome Analysis Toolkit
GlpK	Glycerol Kinase
H_2O	Water
HisG	ATP Phosphoribosyltransferase
HTS	High Throughput Screening
ICL	Isocitrate Lyase
InDel	Insertion/Deletion
INH	Isoniazid
K_i	Enzyme Inhibition Activity
KAN	Kanamycin
kg	Kilogram
LC-MS	Liquid Chromatography – Mass Spectrometry
LEV	Levofloxacin
M. smegmatis	*Mycobacterium smegmatis*
M. tuberculosis	*Mycobacterium tuberculosis*
MDR-TB	Multidrug-resistant Tuberculosis

mg	Milligram
$MgCl_2$	Magnesium Chloride
MGIT	Mycobacteria Growth Indicator Tube
MIC	Minimum Inhibitory Concentration
ml	Millilitre
mm	Millimetre
MOX	Moxifloxacin
MQ	Menaquinone
MmpL2	Mycobacterial Membrane Protein Large 2
MmpL3	Mycobacterial Membrane Protein Large 3
MmpL4	Mycobacterial Membrane Protein Large 4
MmpL5	Mycobacterial Membrane Protein Large 5
MmpS5	Mycobacterial Membrane Protein Small 5
MTZ	Metronidazole
NaCl	Potassium Chloride
NDH-1	Mycobacterial Type I NADH Oxidoreductase
NDH-2	Mycobacterial Type II NADH Oxidoreductase
nm	Nanometre
NMR	Nuclear Magnetic Resonance
OADC	Oleic Albumin Dextrose Catalase
OD	Optical Density
OD_{600}	Optical Density at 600 nanometres
OFL	Ofloxacin
PAS	Para-aminosalicylic acid
PCR	Polymerase Chain Reaction
PDIM	Phthiocerol dimycocersate
PZA	Pyrazinamide

RFB	Rifabutin
RIF	Rifampicin
RNA	Ribonucleic Acid
ROS	Reactive Oxygen Species
SAR	Structure-Activity Relationship
SDS	Sodium Dodecyl Sulphate
siRNA	Small Interfering Ribonucleic Acid
SNP	Single Nucleotide Polymorphism
SSPE	Saline Sodium Phosphate-EDTA
STR	Streptomycin
TB	Tuberculosis
TBE	Tris-Borate- EDTA
TE	Tris-EDTA
TraSH	Transposon Site Hybridisation
V	Volt
vcf	Variant Call Format
WHO	World Health Organization
XDR-TB	Extensively Drug-Resistant Tuberculosis
ZN	Ziehl-Neelsen

Chapter 1

General Introduction

1.1. Background

The *M. tuberculosis* genome undergoes spontaneous mutations and drug resistance clones are selected during monotherapy (1), necessitating the use of a multi-drug regimen. The current multi-drug regimen consists of a two month intensive phase of therapy, followed by a four month continuation phase. Drugs used during the intensive phase include isoniazid (INH), rifampicin (RIF), ethambutol (EMB) and pyrazinamide (PZA), while the drugs used in the continuation phase only consist of INH and RIF. These four drugs are considered first line drugs (Figure 1.1), but when RIF resistance is detected, the regimen is adapted appropriately to include second line drugs, such as amikacin (AMK), kanamycin (KAN), and ethionamide (ETH) (2).

Table 1.1: First and second-line drugs used in the TB treatment regimen.

First Line Drugs	•Isoniazid •Rifamipicin •Ethambutol •Pyrazinamide
Second Line Drugs	•Fluoroquinolones (Moxifloxacin, Ofloxacin, and Levofloxacin) •Aminoglycosides (Kanamycin and Amikacin) •Thioamides •Pyrazinamide •Terizidone

Treatment outcome of patients with resistance are poor (3–5) and are often associated with acquisition of additional resistance. Most recently, cases resistant to all available drugs have been reported (6). This increase has initiated the search for new drugs and repurposing of drugs used to treat other infections (7, 8). Although major investments are made in the development of new drugs, only a few drugs reach the market, such as bedaquiline (BDQ), a drug with a novel target within *M. tuberculosis*. This is the first novel drug to be approved by the Food and Drug Administration (FDA) in 40 years. According to the Working Group on New TB Drugs; various new anti-TB drugs, as well as repurposed drugs, are currently in clinical trials against TB.

It is important to establish the potential risks for drug resistance against the drugs that pass these clinical trials. Uncovering possible resistance mechanisms will assist the development of rapid and efficient diagnostic tests for the new or repurposed drugs.

An example of a drug currently being repurposed for drug-resistant TB is clofazimine (CFZ). It belongs to the riminophenazine structural family and was developed for TB treatment (9), but the side effects of gastro-intestinal irritation, eosinophilic enteritis and blue-red skin discolouration led to the discontinued use of CFZ against TB. CFZ is currently used against leprosy, and it is rare that drug resistance arises (10). The bactericidal/static activity of CFZ against *M. leprae* is high, while the activity against *M. tuberculosis* has shown promise in *in vitro* and murine models (11).

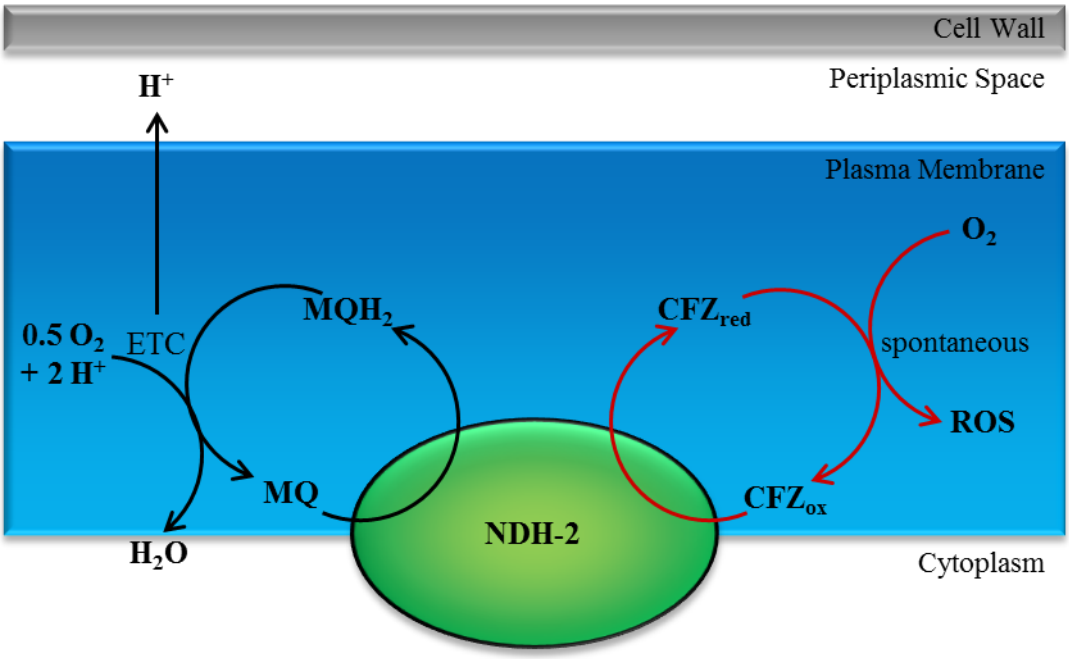

Figure 1.1: A schematic represenation of CFZ competing with menaquinone (MQ) for reduction by NDH-2 in *M. smegmatis*. Reduction of MQ forms part of the electrons transport chain (ETC) in the organism. The reduction of CFZ leads to the formation of reactive oxygen species (ROS). (Adapted from (12))

The mechanism of action of CFZ against *M. tuberculosis* has not been established, but it has been suggested that it may play a role in redox reactions. Reduction of CFZ was reported in 1957, when *M. tuberculosis* grown in aerobic conditions in the presence of CFZ turned reddish in colour, and when switched to anaerobic growth conditions returned to colourless (12). The Yano et al. (2011) study showed that mycobacteria treated with CFZ results in the production of reactive oxygen species (ROS) through a cyclical pathway fuelled by O_2 and

NADH (12). The continual production of NADH by fatty acid β-oxidation and/or the citric acid cycle will drive the cycle, driving the production of ROS. It has been shown in *M. tuberculosis* and *M. smegmatis* that a mycobacterial type II NADH oxidoreductase (NDH-2) "is the only oxidoreductase mediating the transfer of NADH electrons/H^+ to the respiratory chain" (12). This may explain why it was difficult generate CFZ resistant *M. tuberculosis in vitro* (12).

At the start of this study not much was understood about the mechanism of resistance against CFZ *in vitro* or *in vivo*.

1.2. Problem Statement

The mechanism(s) whereby *M. tuberculosis* develops CFZ resistance is poorly understood.

1.3. Hypothesis

Mutations which cause CFZ resistance and do not severely affect growth phenotype *in vitro* will predominate in CFZ resistant clinical isolates.

1.4. Overall Aim

To identify mutations causing CFZ resistance.

1.4.1. Specific Aim 1

To generate CFZ mono-resistant mutants *in vitro*.

1.4.2. Specific Aim 2

To identify phenotypic differences between the progenitor and the CFZ mono-resistant mutant through growth analysis, cell and colony morphology and minimum inhibitory concentration determination.

1.4.3. Specific Aim 3

To identify genomic differences between the progenitor and the CFZ mono-resistant mutant.

Chapter 2

Literature Review

Preclinical and Clinical Anti-Tuberculosis Drug Development

2.1. Introduction

Prior to the antibiotic era, during the early 1900's, tuberculosis (TB) was a major cause of death, especially during World War II within concentration camps (13, 14). Mathematical models indicate a steady decline in the incidence of respiratory TB, before the discovery of streptomycin (STR) in 1944 (15). It is suggested that this decline was due to the development and improvement of health care facilities (16, 17). Importantly the discovery and implementation of STR in the TB treatment regimen resulted in a noticeable decrease in mortality rates of TB patients (17).

The first cases of TB mortality due to the development of STR resistant *M. tuberculosis* strains were reported in 1948 by the British Medical Research council (18). Alternative treatment options for patients with STR resistant TB included the administration of para-aminosalicylic acid (PAS), as it was shown that STR resistant *M. tuberculosis* was sensitive to PAS (19). The discovery of STR and PAS was followed by isoniazid (INH) (20), pyrazinamide (PZA) (21) and cycloserine (CYC) in 1952 (22). Development of additional drugs followed slowly until 1996 (Table 2.1), but renewed research focus and funding has led to the development of several new promising candidates that have not been approved for use by humans (22).

To prevent the emergence of drug resistance, current regimens employ multiple drugs to enhance killing via different targets and mechanisms of action. The standard drug therapy regimen for drug susceptible TB, is divided into two phases. The first phase is a two month intensive phase treatment with INH, rifampicin (RIF), PZA and ethambutol (EMB) (Table 2.1). This is followed by a continuation phase of treatment with INH and RIF for four months. Upon identification of drug resistance to the first-line drugs, second-line drugs (Table 2.1) are administered.

Directly Observed Therapy – Short Course (DOTS) was the first strategy implemented globally to control the transmission of TB (23). DOTS was based on five key elements; (i)

commitment from the government to maintain TB control, (ii) use of sputum-smear microscopy to diagnose patients, (iii) observation of treatment, (iv) a functional supply of drugs, and (v) a standardised system to record and report the results (23, 24).

Table 2.1: Information regarding the current drugs used against *M. tuberculosis.*

Drug	Year Discovered	Target	Mechanism of Action	Resistance Causing Mutation	References
First Line					
STR	1944	16S rRNA	Protein translation disruption	*rrs*, *rpsL*	(25)
INH	1952	InhA	Inhibit mycolic acid synthesis	*inhA*, *inhA* promoter, *katG*, *ndh*, *ahpC*, *kasA*	(26, 27)
PZA	1952	RpsA and FASI pathway	Blocks trans-translation	*pncA*, *rpsA*	(28)
EMB	1961	Arabinosyl transferase	Inhibit cell wall arabinogalactan synthesis	*embB*	(29, 30)
RIF	1963	RNA polymerase	Inhibit transcription	*rpoB*	(27, 31)
Second Line					
CYC	1952	D-alanine ligase	Inhibit D-alanine racemase and D-alanyl-D-alanine synthetase	*cycA* (suspected)	(32, 33)
ETH	1956	InhA	Inhibit mycolic acid synthesis	*ethA*, *ethR*, *inhA* and *inhA* promoter	(34)
KAN	1957	16S rRNA	Inhibit protein transcription	*rrs*	(29)
CAP	1963	16S rRNA	Inhibit protein transcription	*tlyA*	(29)
AMK	1972	16S rRNA	Inhibit protein transcription	*rrs*	(29)
LEV	1986	DNA gyrase & DNA topoisomerase	Inhibit DNA gyrase	*gyrA*, *gyrB*	(35)
PAS	1944	Unknown	Unknown	*thyA*	
OFL	1982	DNA gyrase & DNA topoisomerase	Inhibit DNA gyrase (36)	*gyrA*, *gyrB*	(36)
GAT	1992	DNA gyrase & DNA topoisomerase	Inhibit DNA gyrase	*gyrA*, *gyrB*	(37)
MOX	1996	DNA gyrase & DNA topoisomerase	Inhibit DNA gyrase	*gyrA*, *gyrB*	(37)

FASI, fatty acid synthase I; ETH; ethionamide; KAN: kanamycin; CAP: capreomycin AMK: amikacin; RFB, rifabutin; LEV, levofloxacin; OFL: ofloxacin; GAT: gatifloxacin; MOX: moxifloxacin

In 2006, the World Health Organization (WHO) launched the Stop TB Strategy. This strategy aimed to (i) expand and enhance the DOTS strategy, (ii) address challenges such as TB/HIV and multidrug-resistant tuberculosis (MDR-TB), (iii) strengthen health systems, (iv) involve all care providers, (v) empower TB patients and communities, and (vi) enable and promote

TB research (38). The subsequent implementation of the DOTS-Plus strategy aimed to control MDR-TB by subjecting suspect MDR-TB patients to drug susceptibility tests (DSTs), followed by treatment with second line drugs if the MDR-TB status was confirmed. Since the implementation of DOTS and the Stop TB strategy, in the mid-1990s, 56 million people have been successfully treated, saving 22 million lives (2).

However; this has not prevented the development of MDR-TB and extensively drug-resistant TB (XDR-TB). *M. tuberculosis* is classified as MDR-TB when the strain is resistant to at least two of the first-line anti-TB drugs INH and RIF. In the case of XDR-TB, the isolate is resistant to INH and RIF in addition to any fluoroquinolone and at least one of the injectable drugs; amikacin (AMK), capreomycin (CAP) and kanamycin (KAN) (39). The emergence of drug resistance negatively influences the control of TB and thereby emphasizes the need for the development of new anti-TB drugs and treatment regimens.

The need for new drugs or re-evaluation of existing drugs is fuelled by the increasing emergence of drug resistant TB and the lengthy treatment duration. Shorter drug treatment would help to reduce non-compliance, thus positively influencing TB control. Few studies focus on repurposing drugs, exceptions include fluoroquinolones that were originally used against other bacteria are now used as in TB treatment and CFZ which is currently being re-evaluated to be used against drug resistant TB. This review will describe current drug development strategies; highlight the advantages and limitations of these approaches, and their application in the identification of potential drug targets and compounds.

2.2. Drug Development

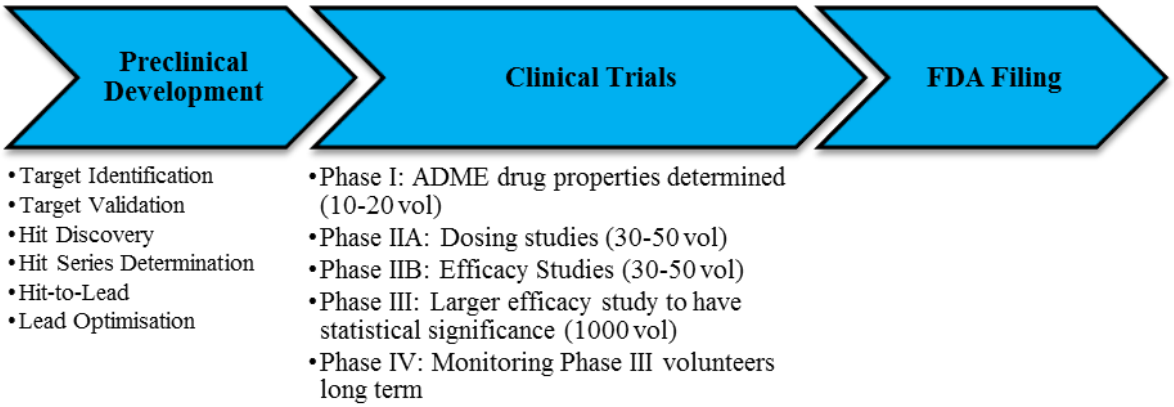

Figure 2.1: A summary of the drug development process. The drug development process is divided into three phases, starting with preclinical development, and if a drug is identified during this step it moves on to clinical trials. If the drug passes these trials it is filed and approved by the Food and Drug Administration (FDA) Vol: volunteers

The development of a new drug is a lengthy process, illustrated in Figure 2.1. A limited number of compounds complete all the mandatory steps and stringent quality control measures for pre-clinical and clinical implementation. Potential anti-TB compounds should (i) target actively replicating cells as well as dormant and persister cells, (ii) have novel targets to combat MDR- and XDR-TB, (iii) shorten therapy time by being more potent, (iv) have no negative interactions with other anti-TB drugs and (v) should be compatible with anti-retroviral treatments, since many patients are HIV co-infected (40).

2.2.1. Preclinical Drug Development

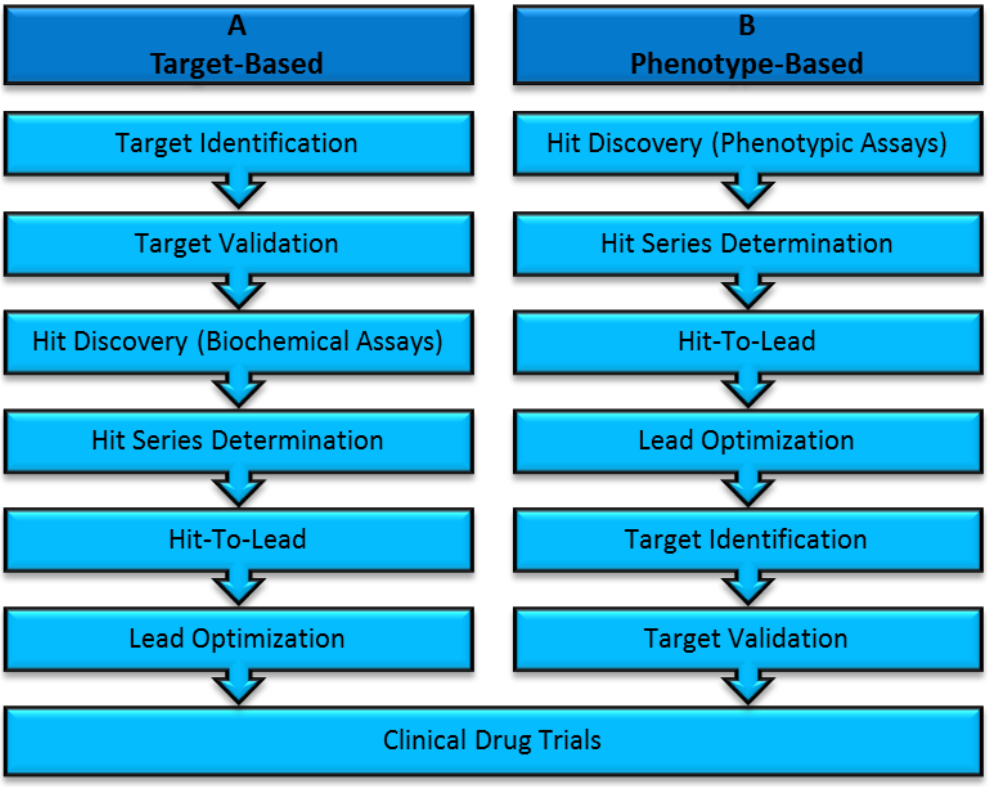

Figure 2.2: Two preclinical drug development approaches. During A which is the target-based approach, the target is identified and validated, and then the compound is identified through biochemical assays, followed by further drug development. B is phenotype-based, where the compound is identified when it has the desired phenotypic effect, and it is developed further from there.

Preclinical drug development is categorized into two approaches. The first is a phenotype-based approach (forward chemogenomics) (Figure 2.2B), where the effects of new compounds are tested on the bacterium to find the desired phenotype. This is followed by target identification and validation (Figure 2.2), to understand the mechanism of action. The

second is a target-based approach (reverse chemogenomics) (Figure 2.2A), starting with identification and validation of protein and nucleic acid drug targets, followed by assays to search for candidate compounds. Mechanisms of actions studies will follow to eliminate redundancy in targets. Here the different steps will be described following the target-based order of events, but would be applicable (in reordered sequence) to the phenotype-based approach.

2.2.1.1. Target Identification

Identification and validation of a new drug target within the bacterium is very important since the target itself determines the efficacy of the new drug. A biological response that can be measured *in vivo* and *in vitro* should be observed when the potential compound is able to bind to the target. A good drug target will form part of an essential pathway within the bacterium, where the inhibition of its activity or disruption of its function will lead to the death of the bacterium. The new drug should have high specificity and affinity for the target. The drug must be efficient, meet the commercial and clinical needs, and must preferentially not elicit adverse effects in the host. The target should be novel to avoid the chance of cross-resistance between a new drug candidate and currently used drugs.

Different approaches can be used to identify new drug targets within the bacterium, such as random mutagenesis where the significance of a metabolite for bacterium survival is determined. The random mutagenesis approach has been used efficiently for the identification of genes that affect virulence or growth of *M. tuberculosis* when the gene is disrupted (41, 42). An example of random mutagenesis used for *M. tuberculosis* is transposon site hybridisation (TraSH), which investigates the essentiality of genes under different conditions (42).

Another approach is compound identification where the effect of a compound on the bacterium is determined; subsequently the compound's mode of action is determined. These compounds can come from either natural products or chemical libraries. After identifying a potential compound by minimum inhibitory concentration (MIC) in media with different carbon sources, the compound is further characterized by mutation frequency determination and subsequent mutant generation. During this approach a compound's target is identified using chemogenomics, which includes drug resistant isolates undergoing DNA sequencing, whole transcriptome analyses and macromolecular synthesis of DNA, protein, RNA, fatty acids and peptidoglycan being assayed (43).

There are numerous criteria that have to be overcome following the identification of a crucial drug target. These include the following; i) the metabolite, transcribed by the target, must be required for infection of the host, not only made during certain disease states, ii) the bacterium should not be able to procure the metabolite from the host and iii) the metabolite should not be synthesised through other pathways to supplement the loss of the metabolite within the bacterium (43, 44). Genetic analyses are not able to provide all the necessary insight regarding the need a bacterium has for a particular metabolite. Other techniques which will help determine the necessity of the metabolite, includes systems biology, imaging *in vivo* and *in vitro*, metabolic modelling and profiling the cell content of the bacteria (45–48).

2.2.1.2. Target Validation

Different models exist to validate a drug target, ranging from *in vitro* culture-based models to *in vivo* modulation in disease patients. For example PA-824, a nitroimidazopyran, was tested *in vitro* using MDR-TB clinical isolates and *in vivo* using a murine model for infection, displaying high activity against *M. tuberculosis* (49). Using multiple validation techniques increases the confidence of the observed outcome. Different validation techniques include the use of monoclonal antibodies, antisense technology and small interfering RNA (siRNA). By using a variety of tools the cellular function of the target is evaluated and validated before investing and committing to screening potential hits.

Monoclonal antibody validation can occur *in vitro*, where the antibody sequences are selected from a variable immunoglobulin region complementary DNA (cDNA) library, or *in vivo*, where host animals are immunised and hybridoma techniques are used to screen for the monoclonal antibodies (50). During antisense validation an antisense RNA oligonucleotide construct is delivered into the cell and the effects on messenger RNA (mRNA) expression measured. In the case of *ilvD*, which plays a role in isoleucine and valine biosynthesis in *M. tuberculosis*, it was found that after the addition of a plasmid with an antisense mRNA oligonucleotide the growth of *M. tuberculosis* in the lungs decreased noticeably in a murine model (51).

It is important to select the right model, since previous studies have shown that different models may have different results. For example, metronidazole (MTZ) is able to kill *M. tuberculosis* under *in vitro* hypoxic conditions in rabbits but not under aerobic conditions (52). However, MTZ is ineffective in killing off *M. tuberculosis* infections in guinea pigs and mouse models (53, 54). While the administration of MTZ for two months to *M. tuberculosis*

infected macaques was as effective as a combination treatment of INH and RIF in preventing reactivation of a latent infection (55).

2.2.1.3. Hit Discovery

A hit is defined as a compound that exerts the preferred activity during compound screening and retesting (56). Compounds that have the potential to become hits are from different origins, including antibiotics that occur naturally, the synthesis of novel chemical compounds and the repurposing of existing drugs used against other bacteria.

Natural drug discovery, where the compounds already exist within nature, started with penicillin discovery by Alexander Fleming in 1929 (57, 58). Since then it has been the cornerstone of novel drug discovery (59). Currently, the marine environment is a major source of natural antibiotics, compounds are isolated from bacteria, fungi and sponges (60). Compounds can be chemically synthesised and altered to design a successful hit, using techniques such as focused screening.

The assays used to screen the identified compounds are normally cell-based, with nuclear receptors, ion channels and membrane receptors as drug targets. The other are biochemical assays which are used with enzyme and receptor targets, but often it merely measures the affinity of a test compound for the target protein. Assays are developed with certain requirements in mind, i.e. the relevant pharmacokinetics, reproducibility, low cost, high quality and the effects the compounds have in the assay (56). Table 2.2 illustrates the preclinical drug development sequence from hit discovery through to lead optimization.

The carbon sources used during assays may play a role in the targets identified as viable candidates. When *M. tuberculosis* is grown *in vitro* the carbon sources used in the media are not the same as that available *in vivo* (61). An example was where an *in vivo* study identified isocitrate lyase (ICL) as a viable target in *M. tuberculosis*; while *in vitro* ICL is unnecessary for the survival of the bacterium (62). This study showed ICL chemical inhibition was dependent on propionate (C_3) and polyoxyethylene sorbitan monolaurate (C_{12}), while glycerol and glucose restored the growth of *M. tuberculosis* (62).

The most recently approved anti-TB drug, bedaquiline (BDQ) (formerly TMC207 and R207910) was discovered during a whole cell assay, using *Mycobacterium smegmatis* as the test organism (63). A whole cell assay was preferred since it enables the assessment of multiple targets within the bacterium. BDQ, part of a chemical class diarylquinolines, showed

the most potent inhibition of *M. tuberculosis*, by inhibiting the bacterial ATP synthase (63). After being described for the first time in 2005, the drug was approved as an anti-TB drug in 2012 by the Food and Drug Administration (FDA).

Table 2.2: The target-based preclinical drug development sequence.

Hit Discovery	Hit Series Determination	Hit-to-Lead	Lead Optimization
• HTS • Focused screening • Fragment screening • Virtual screening • Physiological screening • NMR	Hits grouped according to SAR	• Hit fragmentation • Bioisosteric replacement • Hit evolution	• Ames test • Irwin's test • Dose linearity • High-dose pharmacology • PK/PD studies • Pharmacokinetic repetitive dosing • Profiling drug induced metabolic processes

One of the routes that can be followed during drug development, starting with hit discovery, followed by hit series determination, hit-to-lead and finally lead optimization. After passing all these steps, the drug goes through to clinical trials. HTS, high throughput screening; NMR, nuclear magnetic resonance and SAR, structure-activity relationship.

High Throughput Screening

Large numbers of compounds can also be screened using high throughput screening (HTS) where the compounds are analysed using a 384 well plate (64). To select which compounds to include during the screening, a database of compounds is initially screened for potency against *M. tuberculosis*. The compounds that show possible interaction are further filtered using Lipinski's rule of five; discarding the compounds with a molecular weight of more than 500, more than five donors of hydrogen bonds, with a lipophilicity value less than five and more than 10 possible hydrogen accepting atoms that could form hydrogen bonds (65). A study, done in 2012, investigated 20 000 compounds using HTS (66). As expected, from these 20 000 compounds, only two were found to be effective against *M. tuberculosis* as well as adhered to Lipinski's rule of five. One of these compounds (a benzimidazole) targets mycobacterial membrane protein large 3 (MmpL3), which is a putative cell wall mycolic acid transporter (66). The other drug is a nitrotriazole which targets the decaprenylphosphoryl-β-D-ribose 2'-epimerase (DprE1), which is required in cell wall biosynthesis (66).

Identification of potential novel drug compounds within a large amount of compounds can be supported with visual assistance, for example a high-content screen (HCS). A HCS is where an ArrayScan™ System is combined with reagents that are fluorescence-based to determine

the roles targets play cell functions (67). During a HCS screen, of 57 000 small molecules, 135 compounds were found to be active against *M. tuberculosis* and displayed no toxicity to the host cell (68). Dinitrobenzamide derivatives (DNB) which showed high activity against *M tuberculosis* were also found to be effective against XDR-TB (68). *M. tuberculosis* treated with DNB demonstrated the inhibition of arabinogalactan and lipoarabinomannan formation, which can be attributed to the inhibition of decaprenyl-phospho-arabinose synthesis catalysed by decaprenyl-phosphoribose 2' epimerase DprE1/DprE2 (68).

Another approach is a luciferase assay which measures the transcription of the *iniBAC* operon (69, 70). The *iniBAC* operon is expressed when drugs are administered to the mycobacterium, inhibiting cell wall biosynthesis (69, 70). Potential compounds active against *M. tuberculosis* cell wall biosynthesis can be identified through measuring the transcription of the *iniBAC* operon. This will also enable the detection of possible cross-resistance between currently used drugs and the potential compounds that both act on cell wall biosynthesis.

Recent advances in liquid chromatography - mass spectrometry (LC-MS) has enabled its use in HTS. LC-MS can be used to determine if a potential compounds can be metabolised by the bacterium (71). The compound should not be metabolised by the bacterium, as this would enable the bacterium to survive treatment with the compound.

Focused Screening

Another technique used is focused screening where structures that bear similarity to previously identified compounds are screened against the target (Figure 2.3) (56). Click chemistry can be defined as joining small units, comprising of a few chemical elements, through heteroatom links (C-X-C) to form larger oligomers (72). Following this strategy, a small focused library of 1,2,3-triazoles was designed through click chemistry, and the compounds were tested against *M. tuberculosis* (73). According to *M. tuberculosis* H37Rv MIC tests one of the compounds was five times more active than econazole but equal to RIF, the two control drugs used in the study, suggesting that this compound may be more effective than the existing drugs (73).

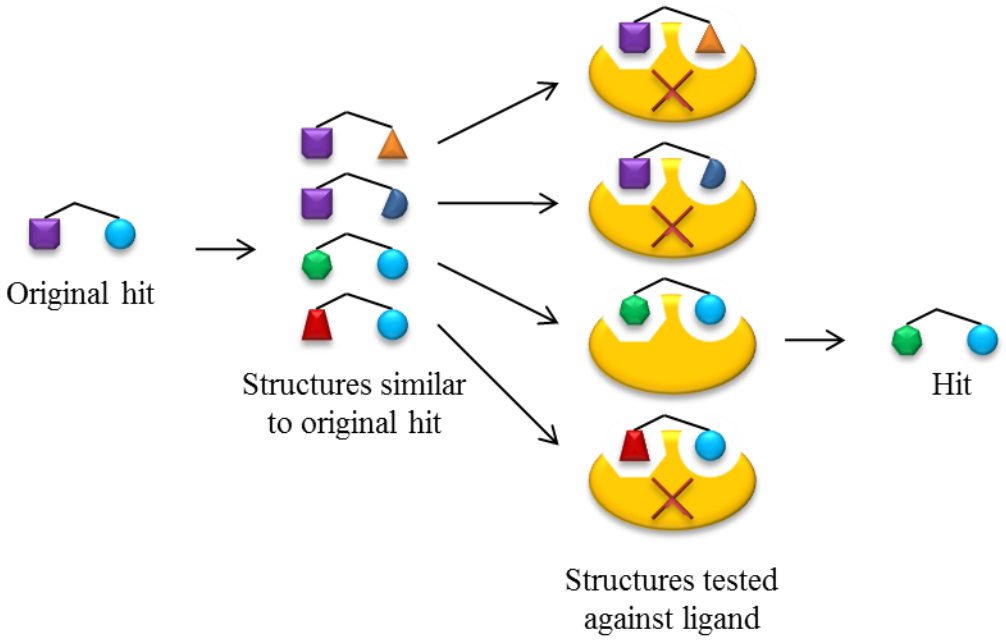

Figure 2.3: Schematic representation of the focused screening technique. Structures that are similar to the original hit are tested against the drug target. Compounds that bind to the target are identified as hits.

Fragment Screening

The fragment screening method consists of three different approaches; virtual screening, nuclear magnetic resonance (NMR) and physiological screening (74). Fragment screening is where compounds, with little complexity (low mM activity), are used for larger molecule building blocks (75).

Virtual Screening

Virtual screening is made possible through the use of X-ray crystallography. X-ray crystallography uses the structure of a protein with a characterised ligand which serves as a base for the identification of compounds that will interact with the protein (Figure 2.4). The biggest disadvantage of virtual screening is that molecular level drug-receptor interactions are too complex for *in silico* hit discovery to be reliable (76). For example, a database containing over 500 000 compounds was virtually screened, in an attempt to find ATP phosphoribosyltransferase (HisG) inhibitors. By using the FlexX and GOLD docking algorithms several compounds were found to have 4-6 µM enzyme inhibition activity (K_i) against HisG, but further experimental procedure, using whole cell assays, were necessary to identify the one compound that was active against *M. smegmatis* (77).

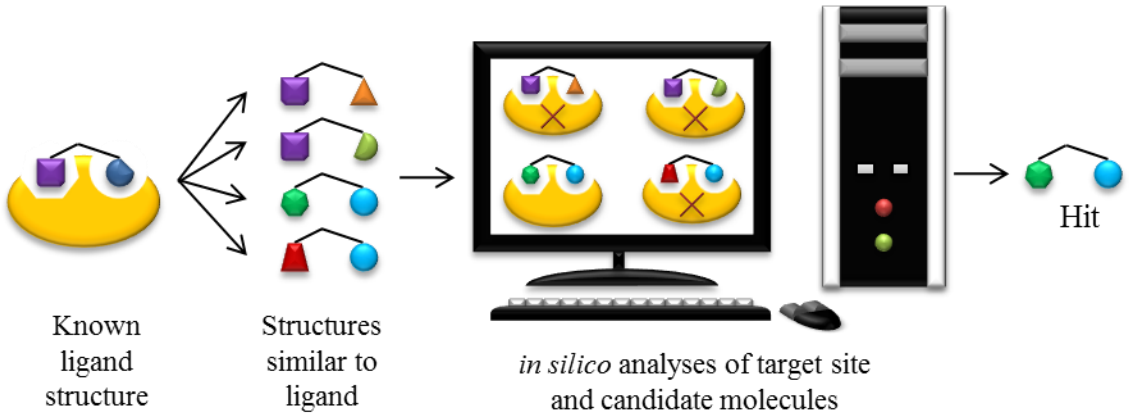

Figure 2.4: The virtual screening process. Structures that are similar to a known ligand which binds to a target is screened *in silico* to identify potential hits.

Nuclear Magnetic Resonance

Magnetic nuclei have different energy levels at different nuclear-spin states when placed in a magnetic field. By applying radio-frequency radiation these magnetic nuclei are enabled to switch between the different energy states, helping to determine the NMR properties of each molecule (78). Small compounds are screened by exposing them to known crystals or NMR protein target structures to identify hits that bind the best (Figure 2.5), but have a low mM activity (78). Hits from NMR screening are subsequently used as building blocks for larger molecules (78).

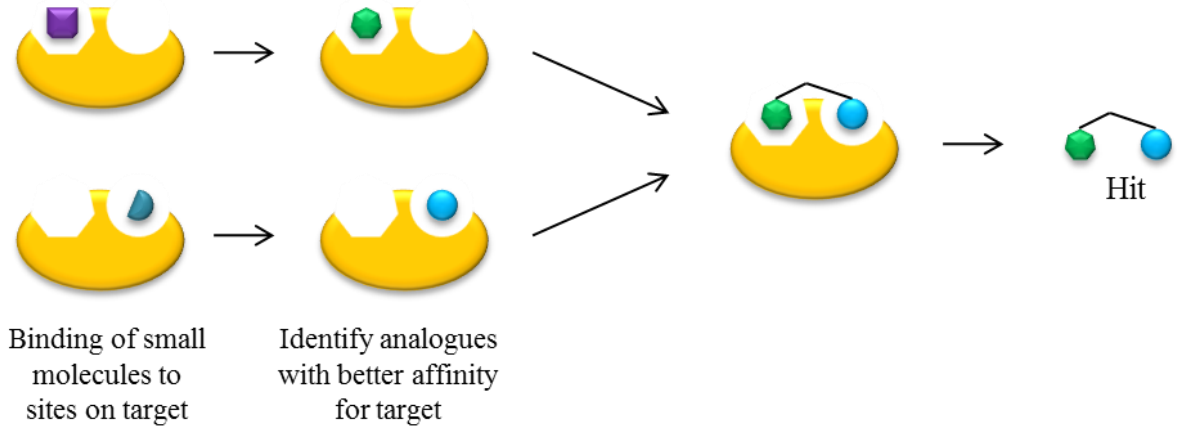

Figure 2.5: Nuclear magnetic resonance. Analogues of small molecules are tested against the target to identify the small molecules that have better affinities for the target. The small molecules with the best affinities are used as building blocks for larger molecules which become hits.

Examples of drugs identified using NMR are the new antimicrobial chemotypes identified in plants, hyperenone A and hypercalin B. Hyperenone A has a growth inhibiting effect on

MurE from *M. tuberculosis* H37Rv (79). There are constant efforts to find inhibitors of Mur enzymes which are essential in the biosynthesis of peptidoglycans, an important component in the *M. tuberculosis* cell wall (80).

Physiological Screening

Physiological screening, displayed in Figure 2.6, is tissue-based where drug effects are determined at a tissue level, rather than cellular or subcellular (56). A clofazimine (CFZ) study, done in mouse models to test the anti-TB activity, showed that a dose of 20 mg/kg daily yielded 0.55 µg/ml plasma concentration, and higher concentrations in the lung and liver (81, 82). This concentration of CFZ is bactericidal, but the onset of the drug is so slow that it may not stop death if the animal is heavily infected (81, 83). This type of screening therefore provides vital information of responses in a more complicated system.

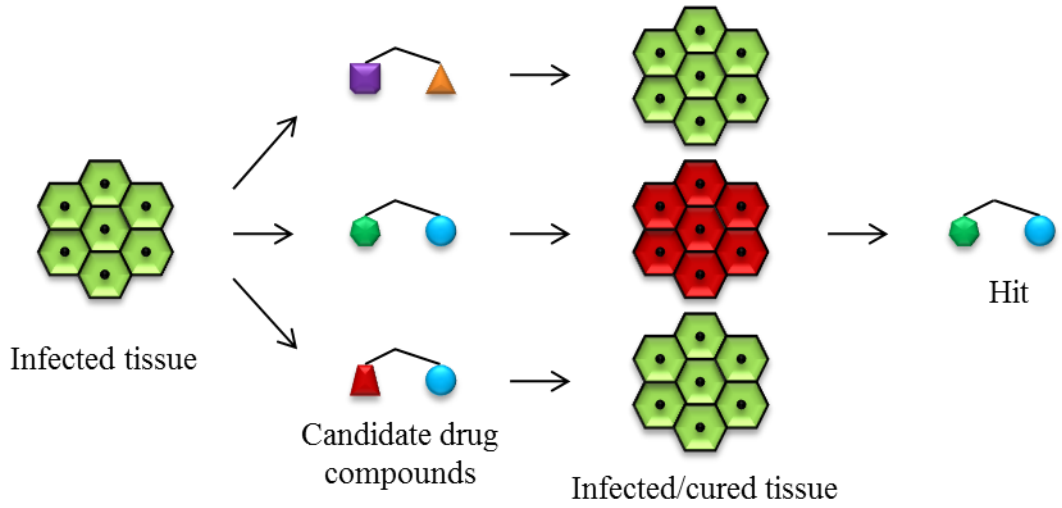

Figure 2.6: Physiological screening. Infected tissue (green) is treated with different candidate drug compounds to find potential hits. If the tissue is still infected (green) following the treatment the compound is discarded from the process. If the tissue is disease free (red) the compound is classified as a hit.

Following the discovery of a number of hits, the drug discovery team must prioritize hits. Firstly, compounds that frequently show up during HTS as false positives are removed and secondly, hits are grouped according to structural similarity by computer algorithms (56). This is followed by measuring dose-response curves, i.e. the response at different dosages, using a fresh sample of the compound. Compounds that have reversible effects would be chosen above compounds that have an all or nothing response, since this would enable the drug to be removed from the patients system after withdrawal of the drug.

Secondary assays are also performed to exclude false positives that were identified during the primary assays (84). The methods used for secondary assays are not the high throughput methods, but focus more on the functional responses the compounds have (56).

2.2.1.4. Hit Series Determination

Hits are grouped into clusters that have structure-activity relationship (SAR) meaning these compounds have some related chemical motif or section of the overall structure. These groups enable testing to be done in parallel, generating SAR data and information of the elements for activity. Representative samples are selected from each group and subjected to an assortment of *in vitro* assays. These assays will provide information about the absorption, distribution, metabolism and excretion (ADME) properties together with pharmacokinetic and physicochemical measurements. Secondary tests can be carried out on these groups to profile the selectivity, especially the original target for which the compounds were made.

The number of hits that move into the hit-to-lead phase should include all the compounds that showed activity to allow for the large loss of hits that occurs during the next phase.

2.2.1.5. Hit-to-Lead

The main aim of experiments done in this phase is to investigate the core of each structure and to measure the selectivity and activity of each compound (56). These investigations are done systematically to improve the SAR, and the availability of structural information improves this process.

Optimization during the hit-to-lead phase depends on the technology used to screen for the hit discovery. The techniques used during the hit-to-lead process (Figure 2.7) may involve hit fragmentation, bioisosteric replacements or hit evolution or combinations of the techniques (85).

Large molecules which have initially been identified by HTS mostly undergo hit fragmentation, which is when the HTS hits are structurally broken down to identify likely minimum ligands or fragments (86–88). New starting points which can be used for fragment expansion can be found by identifying the core fragments of HTS hits that have significant molecular complexity. This strategy has been used successfully to identify metalloenzyme inhibitors in a library screen of chelator fragments.

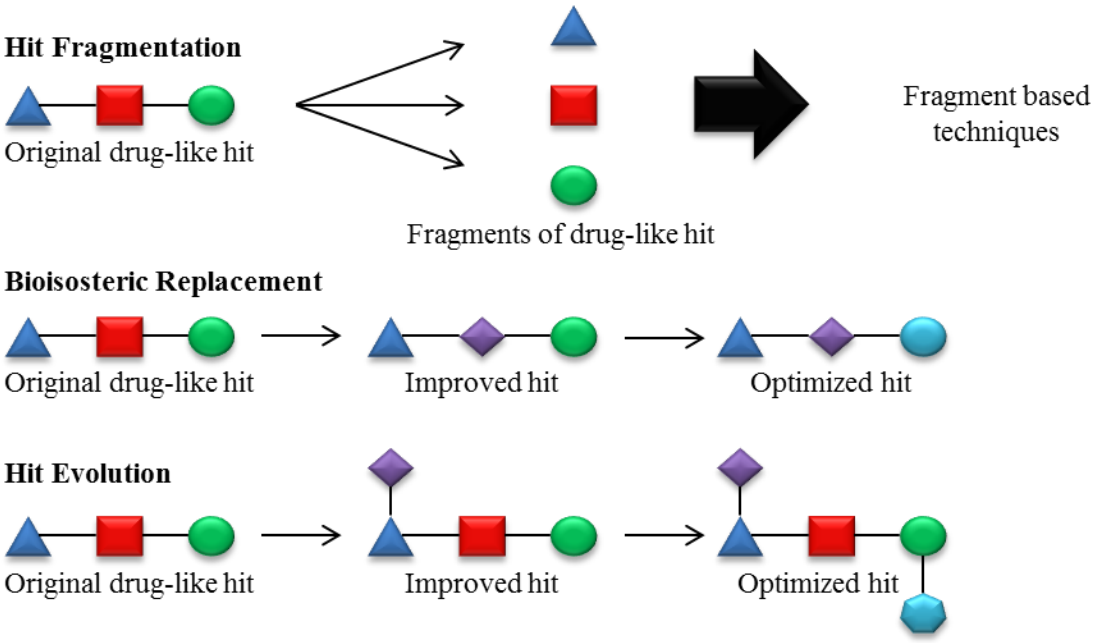

Figure 2.7: A diagrammatic representation of the hit-to-lead approaches explained in this review. During hit fragmentation an original drug-like hit is fragmented to undergo fragment based techniques. Bioisosteric replacement involves replacing a small part of the original drug-like hit to obtain an optimized hit. During hit evolution fragments are added to the original drug-like hit to result in an optimized hit. (Adapted from (85))

Bioisosteric rules are used during the hit evolution technique of bioisosteric replacements. The term refers to two compounds that have a similar shape in a certain biological environment, for example a protein binding site (89). The method of bioisosteric replacements uses this biological similarity where the structure of the target is used to determine the similarity. However, the structure of the target is often not known, restricting the use of this method. In the course of PA-824 synthesis, the drug was insoluble because of a biaryl carbamate moiety, but by replacing the group with an arylpiperazine it resulted in PA-824 being more soluble (90).

During hit evolution, analogues with altered substitution patterns are chemically synthesised from the original hits. To create focused libraries (compound collections) the compounds are synthesised by solution- or solid-phase parallel synthesis, together with high throughput purification to aid the output of compounds for screening. Purified or crude compound analogues that have improved dissociation constants are screened using competitive conditions together with affinity screening methods (91). The SAR data gathered from these libraries can be used for medicinal chemistry exploration, in the hope to produce more

compounds which may have an enhanced lead-like profile, with physiochemical and structural profile of a good lead compound (85).

When hit-to-lead optimization is successful, the drug-like lead compound that results from HTS hits does not depend on the original hit's lead-likeness. According to Keserü & Makara (2006), "chemical similarity between hits and leads derived from them is somewhat larger for HTS hits (average 0.61) than that for fragment-based hits (average 0.56)" (85) The increase in ligand efficiency, i.e. the binding free energy for each heavy atom, of HTS hits during lead optimization is a clear indicator of the value this technique has (85, 92).

Other important factors to consider are permeability and solubility of a drug, since the substance needs to be absorbed in the gastrointestinal tract or may be injected into the circulatory system (56). Unfortunately the amount of drug candidates that have low-solubility has increased, which is a significant problem for pharmaceutical companies performing drug design and development (93).

2.2.1.6. Lead Optimization

The main objective of lead optimization is to improve on the deficiencies of a compound whilst sustaining the favourable properties (56). Upon reaching this phase, the compound may have met all the requirements for lead optimization and can therefore be declared a candidate for preclinical trials. However, synthetic back up molecules need to be created, in case the compound that is undergoing preclinical or clinical characterization is unsuccessful, the back-up candidate can then be evaluated.

Mutagenic qualities of a compound are assayed in the Ames test (94), while the Irwin's test estimates the minimum concentration of a compound that is necessary for it to be lethal (95). Other tests that need to be carried out by the end of this phase are pharmacological studies to determine dose linearity, kinetics and pharmacodynamic properties. The effect of lead molecules on host metabolic processes also needs to be assessed.

Only after all these hurdles have been overcome, the drug can be considered for human clinical trials. The whole process from target identification up to the selection of the preclinical candidate is a lengthy procedure and has no set routine; there are many different routes within this process that can be followed to reach the final preclinical candidate. Each project may start off with 2000 – 5000 compounds and through the preclinical phases only one or two molecules arise as candidates that will enter clinical trials (56).

2.2.2. Clinical Drug Trials

New generation anti-TB drugs must undergo human clinical trials before they can be used in the general population. Clinical drug trials are divided into four phases. During phase I ADME properties of the drug are determined (96, 97). Drugs need to have a high penetration of bacterial cell envelopes, as efficiency is influenced by the amount of drug entering the cell (98).

Initially 3-4 human participants are used to determine side effects of a specific single dose and if no adverse side effects occur the number of patients are increased up to 10 or 20 and the effect of multiple doses studied (97). In the case of the combination of drugs with no side effects, such as the combination of meropenem and clavulanate, the drug could proceed to the next phase (99). In some cases the side effects are manageable; such is the case with CFZ which causes a red-brown skin discolouration, but disappears after drug use is discontinued (100, 101).

Phase II can be divided into two parts. In phase IIA, the dosing studies are done with 30 – 50 participants to determine the optimal dose. Phase IIB comprises efficacy studies which are done to determine efficacy with a larger group of volunteers (200–500) (96, 97). This phase can last as long as up to 2 years to determine if the drug is efficient enough and if there are no long term side effects before going into phase III (97).

Many more volunteers are needed for phase III studies to determine whether the efficacy of the drug shows statistical significance. More than a 1000 volunteers are used to assess if the drug is superior or equivalent to the current drugs but with fewer side-effects (96, 97). This phase is carried out in a clinical hospitals where the previous phases are normally in university or research based hospitals (97). During phase IV, no new tests done on the volunteers, but the previous volunteers are merely monitored to detect an adverse effects that may occur with prolonged use (97, 102).

2.2.2.1. Drugs Currently in Clinical Trials

Currently there are multiple drugs in various phases of the clinical trials. According to the Working Group on New TB Drugs (2014) there are currently no drugs in phase I, while there are several drugs in phase II, including PA-824, Linezolid, SQ-109, AZD5847 and Sutezolid. Among the drugs undergoing phase III trials are gatifloxacin, moxifloxacin, rifapentine and delamanid (OPC-67683). Most of these new drugs have the potential to be used against drug-

resistant bacteria and to shorten treatment time (103). Table 2.3 displays the targets of these drugs however, not all of the targets have been determined.

Table 2.3: Targets of drugs currently in clinical trials for TB therapy

Drug	Phase (104)	Target
AZD5847	IIA	50S Ribosomal Unit
Bedaquiline	IIB	c Subunit of ATP Synthase
PA-824,	IIA	Mycolic Acid Biosynthesis
Linezolid, PNU-100480	IIA	50S Ribosomal Unit
SQ-109	IIA	Arabinogalactan
Sutezolid	IIA	50S Ribosomal Unit
Gatifloxacin, Moxifloxacin	III	DNA gyrase
Rifapentine	III	RNA polymerase
Delamanid (OPC 67683)	III	Mycolic Acid Biosynthesis

Adapted from (105)

The Global Alliance of TB Drug Development (TB Alliance) currently has ongoing trials that test the efficacy of different drug regimens (106). CFZ is included in three of the arms of the New Combination 3 (NC003) trial, which is currently in phase IIA (106). The three combinations of drugs include BDQ + CFZ + PA-824 (JCPa), BDQ + CFZ + PZA (JCZ) and BDQ + CFZ + PZA + PA-824 (JCZPa). According to the TB Alliance the regimens are fixed dosages, orally administered, less expensive, can be used with antiretrovirals and show promise in shortening TB treatment to less than four months. However, there are already reports of drug resistance in patients using BDQ. To make matters worse, recent studies have identified cross-resistance between BDQ and CFZ caused by various mutations in *Rv0678* (107–109). The mechanisms of cross-resistance require urgent elucidation, as it has implications for patients with already limited therapeutic options. The development of resistance so soon after introduction into the clinical situation needs urgent attention, particularly in the area of resistance mechanisms and the development of proper diagnostics to identify such resistance. The previously reported change in minimum inhibitory concentration (MIC) was 2 fold (107), which may impede the effectivity of CFZ enough to render it inadequate for successful treatment. The outcome of these studies might result in BDQ and CFZ not being used together in a regimen as in the trials mentioned above.

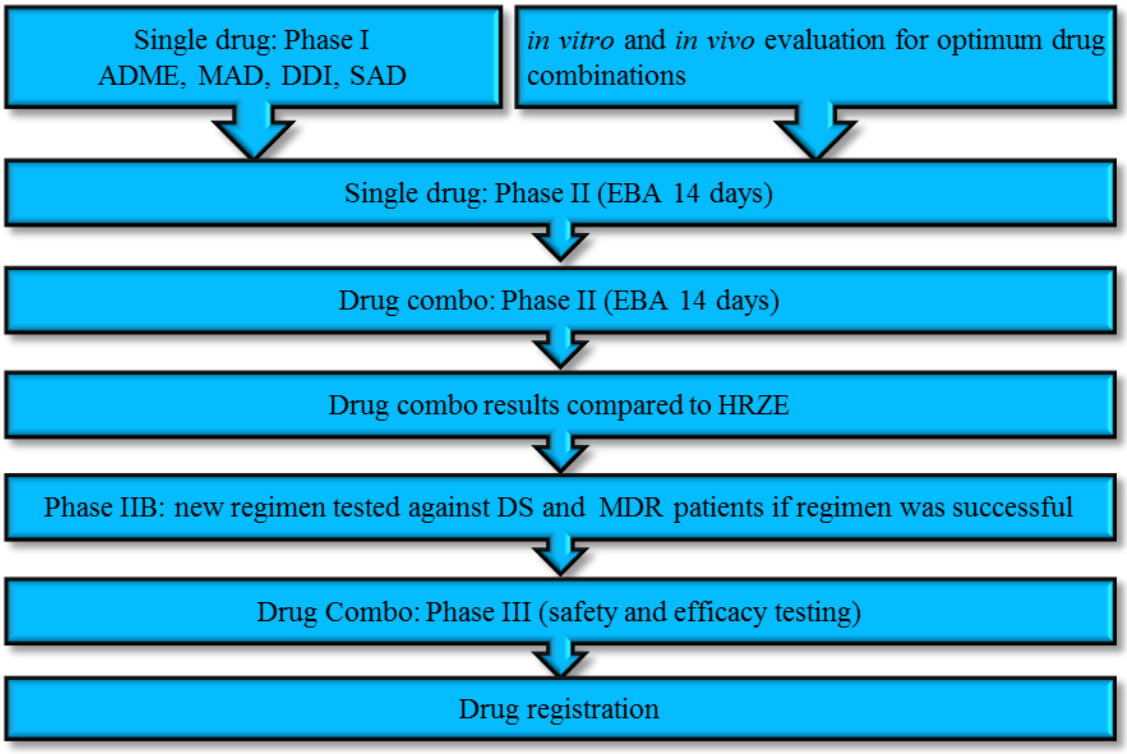

Figure 2.8: New drug development pipeline for anti-TB drugs. HRZE is the standard drug regimen consisting of isoniazid (H), rifampicin (R), pyrazinamide (Z) and ethambutol (E).

A new model has been designed for novel anti-TB drug development, as shown in Figure 2.8, where new promising drugs are tested in combination to shorten the amount of time from hit discovery to approval (110). Phase I trials, which include single ascending dose, multiple ascending dose, drug-drug interaction and ADME assessments, are conducted at the same time as preclinical *in vitro* and *in vivo* evaluations. This is done to determine the optimum candidate drug combinations aimed at shorter therapy time and prevention of relapse. The two parallel trials are followed by an early phase II trial (single drug) where the early bacterial activity (EBA) is determined over 14 days (110). EBA enables rapid detection of the effect a new drug may have using a limited amount of patients, selection of appropriate dosage for further trial experiments and studying of the relationship between bactericidal activity, toxicity of the drug and its pharmacokinetics (111). The use of EBA and pharmacokinetic studies give insight into drug behaviour in humans, such as appropriate dosages (112, 113). Based on the trials completed, a candidate drug regimen is developed and goes on to phase II EBA testing (combo EBA). Results of the phase II EBA testing are compared to the existing regimen of INH, RIF, PZA and EMB; if it was more successful, the regimen progresses to phase IIB where it is tested in drug susceptible and drug resistant TB patients for two months. If the data supports the efficiency of the new regimen, it is brought

into phase III where the safety and efficacy is tested. Currently the TB Alliance is using this model to develop a novel drug combination, to be used against drug sensitive *M. tuberculosis* and MDR-TB, which consists of PZA, MOX and PA-824 (114). A 14-day EBA study of the regimen has been completed, using a the standard regimen of INH, RIF, PZA and ETH as a control (114). This regimen has been advanced to phase IIA.

2.3. Conclusion

The aim of discovering new drugs is to find a drug that shortens anti-TB treatment and has a defined mechanism of action which will combat acquisition of drug resistance. Before a new drug compound is allowed for large scale clinical use it has to undergo the rigorous tests to ensure the safety of patients. These tests take years, and most candidates do not make it to the market, which is one of the most important reasons why there have been so few new drugs in the last three decades.

In December of 2012, for the first time in 40 years, an anti-TB drug, BDQ, was approved for clinical use against MDR-TB (115). BDQ has a novel mechanism of action against *M. tuberculosis*, namely the inhibition of the ATP synthase (116, 117). It is expected that in future, targeting of novel mechanisms of action, particularly those targeting metabolic pathways, will be able to curb the increase of MDR-TB prevalence.

In summary, multiple new or repurposed drugs are currently in clinical trials and will hopefully reach the market in the near future to counter the widespread TB disease.

Chapter 3

Material and Methods

3.1. Clofazimine *in vitro* Mono-Resistant Mutant Generation

A clinical pan-susceptible *Mycobacterium tuberculosis* progenitor, K636, was obtained from a culture bank maintained at the Department of Biomedical Sciences, Stellenbosch University. It was grown at 37^{o}C for seven days in Middlebrook 7H9 broth (enriched with 10% Albumin Dextrose Catalase (ADC), 0.5% Tween and 0.2% glycerol (7H9+ADC)). One-hundred microliter aliquots were then spread plated, in quintuplicate, on Middlebrook 7H10 agar (Becton, Dickinson and Co., Sparks MD, USA) (containing OADC (Oleic Albumin Dextrose Catalase; Becton, Dickinson and Co., Sparks MD, USA) and 2% glycerol), (7H10+OADC), and either 2.6 µg/ml (10× CFZ minimum inhibitory concentration (MIC)) or 2.9 µg/ml of clofazimine (CFZ; Sigma-Aldrich, St. Louis, MO, USA) respectively. CFZ stock solutions were prepared in dimethyl sulfoxide (DMSO; 99%; Merck, New Jersey, USA) at a concentration of 500 µg/ml. To establish viability in the absence of the drug, serial dilutions from the culture were also plated on Middlebrook 7H10+OADC agar without CFZ. Plates were incubated for 30-40 days at 37^{o}C before being inspected for the presence of *M. tuberculosis* colonies.

The colonies observed on the 7H10+OADC plates were cultured in 50 ml tissue culture flasks (Greiner Bio-one, Maybachstreet, Germany), containing 10 ml 7H9+ADC. To exclude colonies that were tolerant, *i.e.* ability to survive in the presence of drug due to adaptive behaviour and not true drug resistance due to mutations, cultures were sub-cultured twice in 10 ml 7H9+OADC without drug. The second set of sub-cultures were standardised to an optical density of 0.2, as measured at 600nm (OD_{600}) in a spectrophotometer (Novaspec II Spectrophotometer, Pharmacia Biotech, England, UK), and exposed to 2.6 µg/ml CFZ for 64 days at 37^{o}C to verify true resistance to CFZ.

Colonies that grew on 7H10+OADC+CFZ agar, were picked and cultured in 7H9+OADC. These clones were stored for further analysis.

3.2. Characterisation of the Clofazimine Mono-Drug Resistant Mutant

3.2.1. Growth Characteristics of Clones

Growth kinetics were established by monitoring the OD_{600} of cultures over time. Selected clones were inoculated into a 10 ml 7H9+ADC starter culture. When these cultures reached mid-log phase, they were used to inoculate 50 ml 7H9+OADC in a 250 ml tissue culture flask (Greiner Bio-one, Maybachstreet, Germany) at 37^{o}C. The starting OD was approximately 0.050 - 0.070, and ODs were measured over a period of 28 days. Growth curves were done in biological triplicate, with technical duplicates of each biological replicate, and the mean OD readings at each time point were plotted on a graph.

3.2.2. Cell and Colony Morphology

Colony morphology was determined by visual inspection to assess colony size, shape, and colour. Cell morphology was determined through Ziehl-Neelsen (ZN) acid-fast staining, and cell shape and colour inspected using light microscopy, using 100× magnification and oil immersion (Olympus CX31,Olympus, Shinjuku, Tokyo, Japan).

3.2.3. Strain Verification Using Spoligotyping

Spacer oligonucleotide typing (spoligotyping) was done as previously described (118), to confirm that the CFZ resistant clones were members of the same family as K636. To amplify the DNA for spoligotyping, each polymerase chain reaction (PCR) consisted of 12.5µl of KAPA Taq 2× Readymix (KAPA Biosystems, Massachusetts, USA), 6.5µl H_2O, 2µl of biotinylated DRa, 2µl of DRb, and 2µl DNA. The concentration of the primer stocks used in the PCR reaction was 5 pmoles/µl for DRa (5'-biotin- GGTTTTGGGTCTGACGAC) and DRb (CCGAGAGGGGACGGAAAC). The thermal cycling profile was 3 minutes at 95ºC, then 30 cycles of 1 minute at 94ºC, 1 minute at 55ºC and 30 seconds at 72ºC, followed by 10 minutes at 72ºC.

Following the PCR, 20µl of the products were added to 160µl of 2× saline sodium phosphate-EDTA (SSPE; 1× SSPE = 1mM EDTA, 10mM NaH_2PO_4 and 0.18M NaCl) which was supplemented with 0.1% sodium dodecyl sulphate (SDS; Merck Laboratories, Saarchem, Gauteng, SA). The diluted PCR product was denatured at 99ºC for 10 minutes, followed by cooling on ice. The nitrocellulose membrane (Ocimum Biosolutions Inc, Hyderabad, India) was washed at 60ºC for 5 minutes with 250ml 2× SSPE-0.1% SDS, placed in a Miniblotter 45 (Immunetics, Boston, Massachusetts, USA) along with a foam cushion, and all extra fluid was aspirated from the channels. The channels were filled with the PCR products, one sample

per channel. Incubation was done at 60ºC for one hour to allow hybridisation of the PCR product to the membrane.

After hybridisation, samples were removed from the miniblotter system by aspiration. The membrane was then removed from the miniblotter and washed twice for 10 minutes each, in 250ml 2× SSPE supplemented with 0.5% SDS at 60ºC. Following the washes, the membrane was incubated at 42ºC for 10 minutes, in 40ml of 2× SSPE-0.5% SDS containing 12µl of streptavidin-peroxidase conjugate (500U/ml stock; Roche, Germany). The membrane was washed twice in 250ml 2× SSPE-0.5% SDS at 42ºC for 10 minutes, followed by rinsing twice with 250ml 2×SSPE at room temperature for 5 minutes. Thereafter the membrane was incubated for one minute in 20ml electrochemiluminescent (ECL) detection liquid (AEC-Amersham Co., Sandton, South Africa), covered with a transparent plastic sheet and exposed to light sensitive X-ray film for two to 20 minutes. The resultant pattern displayed on the X-ray was used to visually identify the strain family to which the clones belonged.

3.2.4. Minimum Inhibitory Concentration Determination in Liquid Media

Drug susceptibility testing (DST) was done using the BACTEC™ MGIT™ 960 system (Becton, Dickinson and Co. Sparks MD, USA). Firstly, liquid cultures were prepared, from glycerol stocks, in 7H9+ADC broth. BACTEC™ MGIT™ Barcoded 7 ml tubes were inoculated with 100 µl from these cultures, followed by the addition of 800 µl of OADC supplement. Growth in the mycobacterial growth indicator tubes (MGITs) was monitored with the aid of the EpiCenter™ Microbiology Data Management System (Becton, Dickinson and Co. Sparks MD, USA). When the starter culture was scored positive (i.e., 400 relative growth units), the tubes were incubated for three more days, whereafter 100 µl was inoculated into new MGIT tubes and the growth process repeated. The new tubes were prepared as illustrated in Figure 3.1, containing drug concentrations of 0, 0.25 µg/ml, 0.5 µg/ml or 1.0 µg/ml. The drug concentrations used during the CFZ MIC determination experiment were calculated using the equations explained in the Addendum to reach the final concentrations of 0.25 µg/ml, 0.5 µg/ml and 1.0 µg/ml.

The MGIT tubes were incubated in the MGIT system at 37^{o}C until the growth control (i.e the 1/100 diluted sample) scored positive. At this point the samples were inspected and scored as sensitive or resistant. Samples with growth units above 100 were scored as resistant, while those below 100 units were scored as sensitive to the particular drug concentrations.

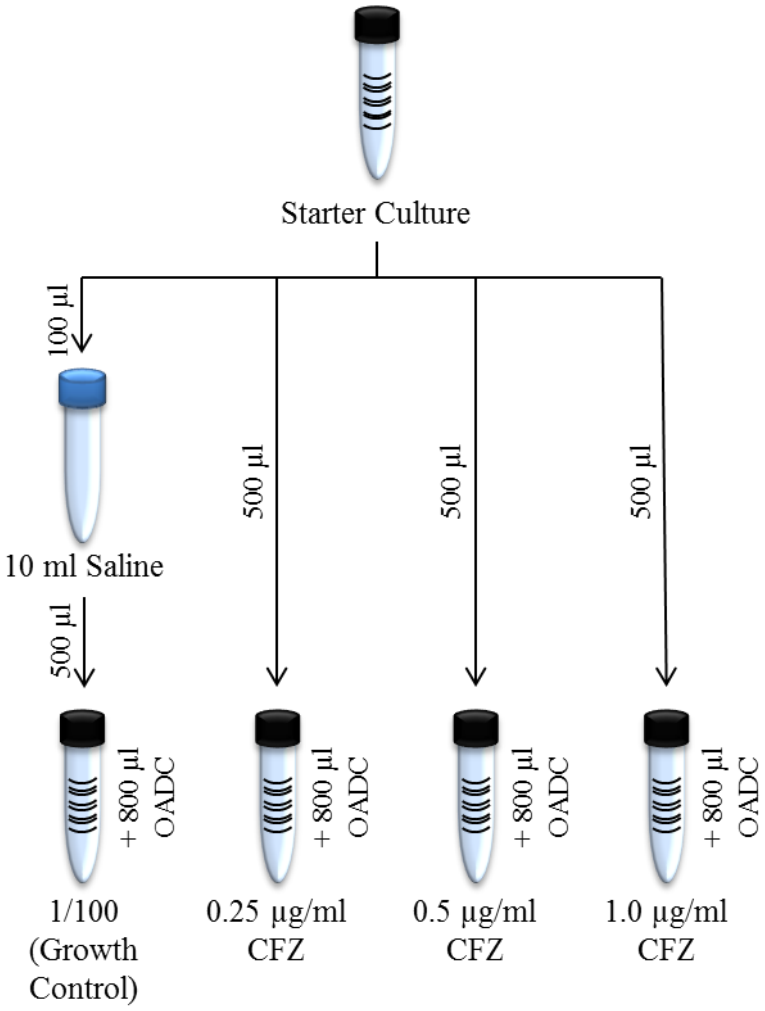

Figure 3.1: A schematic representation displaying the method used during setup for MIC determination in the BACTEC™ MGIT™ 960 system.

3.2.5. Minimum Inhibitory Concentration Determination Using Agar Dilution Method

The MICs of the CFZ resistant isolates were also determined on 7H10+OADC plates containing varying concentrations of CFZ (0.5 µg/ml, 1.0 µg/ml, 2.0 µg/ml, 2.5 µg/ml and 3.0 µg/ml). Three biological replicates were used, each with two technical replicates. Briefly, liquid cultures of the progenitor and CFZ resistant isolates were grown to an OD between 0.5-0.7 before 100 µl aliquots were plated on 7H10+OADC+CFZ and incubated at 37ºC. Dilutions of 1×10^{-6} of the progenitor and CFZ resistant isolates was also plated on 7H10+OADC to determine the colony forming units per millilitre at the time of plating. MIC was defined as the killing off of 99% of the bacteria.

3.3. Whole Genome Sequencing Analysis of Clofazimine Resistant Strains

3.3.1. DNA Extraction

Genomic DNA was extracted as previously described by Warren *et al*., 2006. For this purpose, *M. tuberculosis* K636 and CFZ resistant clones were inoculated into 7H9+ADC broth from frozen stocks, and incubated at 37ºC for 14 days. Sub-cultures from these starter cultures were used to inoculate 7H10+OADC agar in 145x20mm Petri dishes. Plates were incubated at 37ºC for 20 days in order to obtain a lawn of growth on plates. Thereafter the plates were incubated at 80ºC for 30 minutes to heat-kill the *M. tuberculosis* cultures.

To extract the DNA the heat-killed *M. tuberculosis* cultures were scraped with a sterile inoculating loop into a 50 ml Falcon tube containing 6ml extraction buffer (25 mM EDTA, 5% sodium glutamate and 50mM Tris-HCl [pH 7.4]) and 20× 4mm glass beads. Duplicate cultures were pooled together in one tube.

Tubes were vortexed for 2 minutes, to obtain a homogenous mixture, whereafter 500µl lysozyme (100 mg/ml, Roche, Germany) was added to break down the bacterial cell wall. RNA was digested with the addition of 2.5 µl heat treated RNAse A (10 mg/ml, Roche, Germany). The contents of each 50 ml tube were mixed by gentle inversion, followed by incubation for 2 hours at 37ºC. Thereafter the cells were lysed with the addition of 600µl of 10× proteinase K buffer (50mM EDTA, 5% sodium dodecyl sulphate and 100mM Tris-HCl [pH 7.8]) and 300µl of Proteinase K (10 mg/ml, Roche, Germany). Tubes were mixed by gentle inversion and incubated for 16 hours at 45ºC.

Subsequently protein and cell debris were removed by extraction with 5ml of phenol/chloroform/isoamyl alcohol (25:24:1). Briefly, the phenol/chloroform/isoamyl alcohol mixture was added to the proteinase K treated suspension and mixed by gentle and repeated inversion over a period of 2 hours. The aqueous and organic phases were separated by centrifugation (Eppendorf Centrifuge 5810R) at 3000 × g for 20 minutes at room temperature (25ºC). The aqueous top phase (containing the DNA) was transferred to a 50ml tube containing 5ml chloroform/isoamyl alcohol (24:1), mixed and centrifuged at 3000 × g for 20 minutes at room temperature. Finally, the resultant aqueous phase was transferred to a new 50ml tube which contained 600µl of 3M sodium acetate [pH 5.2] and the DNA was precipitated with the addition of an equal volume of cold isopropanol. Precipitated DNA was immediately collected using a glass rod and transferred to a new vial containing 1ml of 70%

ethanol. DNA was then air dried whereafter it was dissolved in 300µl of Tris-EDTA (TE) buffer (1mM EDTA, 10mM Tris-HCl [pH8.0] and stored at -20 º C until further use.

3.3.2. Whole Genome Sequencing

3.3.2.1. MiSeq Illumina Sequencing

DNA from the progenitor (K636) (n=1) and CFZ resistant clones (n=2) were sequenced using the Illumina MiSeq platform with the MiSeq Reagent Kit v3 at the Institute for Microbial Biotechnology and Metagenomics at the University of the Western Cape, South Africa. The MiSeq Kit v3 allows 600 cycles, leading to longer read lengths.

3.3.2.2. Computational Analysis of Whole Genome Sequencing Data

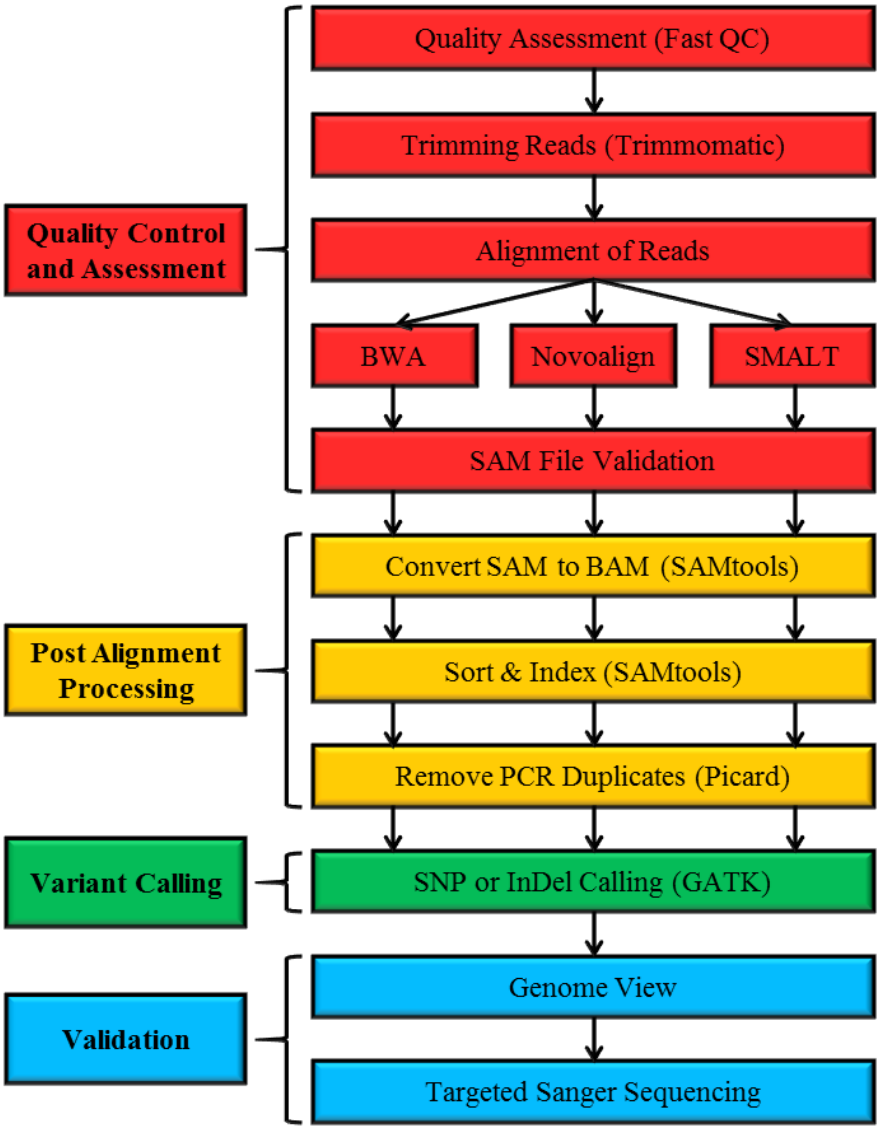

Figure 3.2: The WGS pipeline followed during bioinformatic analyses of the Illumina MiSeq sequencing data.

The MiSeq Illumina sequencing data was analysed in collaboration with Dr RG van der Merwe (Stellenbosch University, RSA) and Dr M de Vos (Stellenbosch University, RSA). An overview of the bioinformatic analysis pipeline that was used is shown in Figure 3.2.

3.3.2.3. Data Source

The genome summary information and genome sequences (in FASTA format) of the reference genome (*M. tuberculosis* H37Rv) were downloaded from GenBank (accession number: AL123456.3) (119).

3.3.2.4. Quality Control and Alignment

Quality Assessment

The quality of the raw sequence reads was validated using Babraham Bioinformatics FastQC software (http://www.bioinformatics.babraham.ac.uk/projects/fastqc/). This is java-based software that outputs HTML files from fastq input files.

Trimming Reads

Trimmomatic v0.32 (120) was used to trim the adaptor and low-quality bases (Quality threshold of 33) from the raw sequence reads. The Phred score used was 33, which allows a 0.0005% chance of error. Error probability in calling bases is logarithmically related to the Phred quality score (Q), for example when $Q = 7\log_{10}$, there is a 1 in 7 chance of error.

The "ILLUMINACLIP" function of Trimmomatic was used with 2 as the maximum amount of mismatches allowed, 30 as the accuracy needed between two reads for palindrome paired-end read alignment and 10 to specify the accuracy needed between any adapter sequence and read to allow it to match.

To trim the bases of low quality from the beginning and end of the read the "LEADING" and "TRAILING" functions were used respectively, keeping any base at the ends of the read with a quality higher than 15.

Through the consideration of multiple bases, referred to as a window, the "SLIDINGWINDOW" function prevents the removal of high quality data in a window containing a single base of poor quality. The quality of a base is determined by the Phred score. The amount of bases included in the window, to average across, was set to 4 and the average required quality was set to 20. Reads that are below a minimal length of 15 were removed using the "MINLEN" function.

Alignment of Reads

Alignments of raw sequence reads were done against the *M. tuberculosis* H37Rv reference genome using three aligners, Novoalign v3-02-04 (http://www.novocraft.com/main/index.php), Burrows-Wheeler Alignment tool (BWA) v0.7.8 (121) and SMALT v0.7.5 (https://www.sanger.ac.uk/resources/software/smalt/#t_1) . The use of three aligners, which apply different algorithms, minimizes the amount of false positives, i.e. bases which are misaligned by a single algorithm. These three aligners produce SAM files which are required to continue through the pipeline.

Novoalign

Novoalign aligns reads generated during Illumina WGS using the Needleman-Wunsch algorithm with gap alignment. The reference genome was indexed using the "novoindex" command with 13 and 1 as the k-mer indexing size and indexing step size respectively.

Burrows-Wheeler Alignment tool (BWA)

BWA aligns short reads to a reference genome (121), in this case *M. tuberculosis* H37Rv. BWA uses Burrows-Wheeler Transform (BWT) with backward search. This tool mimics the digital tree top-down traversal of the genome, using a relatively small amount of memory, counting the exact number of hits a string of a certain length has in a certain time, irrespective of the genome size.

The reference genome was also indexed using the "faidx" function from SAMtools (http://samtools.sourceforge.net). The BWA "aln" command was used to find coordinates of good hits for suffix array (SA) in every read, followed by the "sampe" command which produces a SAM file by converting the SA coordinates into chromosomal coordinates.

SMALT

The reference genome was indexed using the "index" command from SMALT. Subsequently this software uses a banded Smith-Waterman algorithm where the sequence segments from the reference genome are matched to the indexed reads. A reliability score for the mapping of each read is reported along with its best gapped alignments.

SAM file validation

To validate the SAM file, produced during alignment, the Picard v1.107 (http://picard.sourceforge.net) "ValidateSamFile" command was used.

3.3.2.5. Post Alignment Processing

Conversion of SAM to BAM

Using the "view" command from SAMtools, a SAM file post processor, the SAM files were converted to the binary (BAM) format.

Sorting and Indexing of BAM files

To convert the BAM file to a more manageable format the "sort" and "index" SAMtools functions were used.

Local Realignment Around Insertions and Deletions

The Genome Analysis Toolkit (GATK) v3.1-1 (122) was used to realign misaligned reads by insertions and deletions (InDels) within the sequenced genome. Firstly the SAMtools "faidx" command was used to create a FASTA index file for the reference genome. Subsequently a dictionary file was also made using the "CreateSequenceDictionary" command from Picard. To fix misaligned reads, small misaligned intervals are identified using the Realigner Target Creator tool, followed by realignment of identified intervals to the reference genome, using the IndelRealigner tool from GATK.

Realigned BAM files Sorting and Indexing

The "sortsam" function from Picard, and "index" function from SAMtools was used to sort and index the realigned BAM files respectively.

PCR Duplicate Removal

During PCR amplification for library construction the production of duplicate reads may occur. To find and remove these duplicates in the BAM file, the "Mark Duplicates" Picard command was used.

Indexing Realigned BAM file

The realigned BAM file, where the PCR duplicates have been removed, was indexed using the "index" function from SAMtools.

3.3.2.6. Variant Calling

To identify variants, i.e. single nucleotide polymorphisms (SNPs) and InDels in the sequenced genomes, H37Rv was used as a reference. Variants were called using the GATK UnifiedGenotyper tool which produced a Variant call format (vcf) file. The "stand_call_conf" command was used to set the minimum Q confidence to 50, which will allow the variant caller to call variants with a minimum Q value of 50. The "stnd_emit_conf" command was

set to 10, which will allow the variant caller to include variants with a Q value of less than 50 but more than 10. The information pertaining to a variant base which includes the number of reads at that position along with the number of reads which contained the alternative and reference base at the specific position.

3.3.2.7. Extracting Overlapping SNPs from Various Pipelines

The combination of three aligners (Novoalign, BWA and SMALT), with GATK as a variant caller, minimizes the risk of identifying false positive variants as three different pipelines were used for SNP and InDel identification (Figure 3.3) namely Novoalign-GATK, BWA-GATK and SMALT-GATK. Overlapping SNPs generated by the three pipelines were extracted using in-house python scripts (RG van der Merwe, unpublished data). For each aligner a vcf file was created containing the identified SNPs and InDels. Extraction of SNPs and InDels present in all three vcf files identified high confidence SNPs creating a final vcf file. Only variants that were identified in all three pipelines were considered during further analysis.

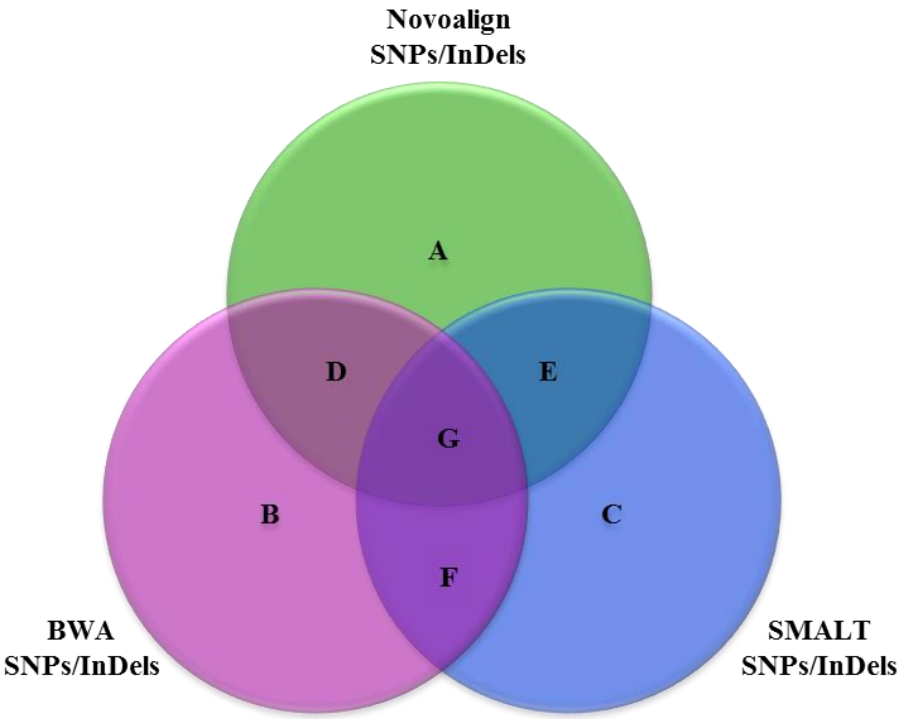

Figure 3.3: A diagrammatic representation of the strategy followed to extract SNPs and InDels. The variants used for further analyses is represented by G, where the SNPs and InDels extracted by (A) Novoalign, (B) BWA and (C) SMALT overlap. The SNPs and InDels identified by only one (A, B or C) or two (D, E and F) aligner(s) are included in the final vcf file, but not investigated further.

3.3.2.8. SNPs/InDels Annotation and Functional Classification

Python scripts were written by Dr RG van der Merwe for; i) annotation of identified SNPs, ii) calculation of predicted amino acid changes for SNPs located within genes, iii) annotation of the identified InDels, iv) calculation of InDel effects on the respective gene's reading frame, and v) classification of the variants according to its cellular function.

3.3.2.9. Validation

GenomeView

The SNPs and InDels that were identified in genomic DNA during variant calling were visualised in each individual read using the GenomeView browser (http://genomeview.org/) graphical user interface. The H37Rv indexed FASTA file was loaded as the reference genome along with the sorted and indexed BAM files from the sequenced genomes. GenomeView shows the aligned reads, hence the amount of reads containing the variant or alternative at a specific base can be visualised.

Validation of Variants Using Sanger Sequencing of Target Regions

Primer Design

Primers were designed, using Primer3 (http://primer3.ut.ee/), to amplify regions containing the identified variants (Table 3.1).

Table 3.1: Primers used for targeted Sanger sequencing.

Target gene		Primer Sequence	Product Size (bp)	T_m (°C)
Rv0678	Forward	5' AAAGCAGTAGGTCAGGGCAT 3'	1147	59
	Reverse	5' CTCGTTGTTGTTGGGCTGG 3'		
Rv2941	Forward	5' CATGAGTGTGCGTTCCCTTC 3'	572	61
(*fadD28*)	Reverse	5' TAACCCGAACGTTCTGATGG 3'		
Rv3696c	Forward	5' CGCCGGCAACTTATTTCTCT 3'	496	61
(*glpK*)	Reverse	5' CACACCGTGGTTAGCAGG 3'		

Polymerase Chain Reaction (PCR) Conditions

PCR reactions were carried out using the Thermal Cycler 2720 (Applied Biosystems, Foster City, CA, USA). Each reaction consisted of 9.375 µl of H_2O, 5 µl 5× Q solution, 2.5 µl 10× µl buffer, 2 µl $MgCl_2$, 4 µl dNTPs (25 mM), 0.5 µl of the forward primer (50 pmol/µl), 0.5 µl of the reverse primer (50 pmol/µl), 0.125 µl HotStarTaq DNA Polymerase (Qiagen, Düsseldorf, Germany) and 1 µl of template DNA. The cycling conditions used were as

follows: (i) denaturing for 15 minutes at 95ºC, (ii) 35 cycles of denaturing for 1 minute at 94ºC, annealing for 1 minute at T_m, extension for 1 minute at 72ºC and (iii) final extension for 10 minutes at 72ºC. A negative control containing no DNA template was included in each experiment.

Gel Electrophoresis

PCR products were prepared adding 5 µl of blue loading dye (0.25% Xylene Cyanol, 30% Glycerol) to 25 µl of the amplification product. Five microliter of each amplification reaction was loaded onto a 1.5% agarose gel. To determine the size of the PCR product, the GeneRuler 100 bp Plus DNA Ladder (Thermo Scientific, Pittsburgh, PA, USA) was loaded into an adjacent well. The amplicons and DNA ladder were electrophoretically fractionated in 1.5% agarose gel (containing 5 µl ethidium bromide (10 mg/ml) per 100ml agarose) and 1× Tris-Borate-EDTA (TBE; 0.45M Tris, 0.44M boric acid and 10mM EDTA; pH8.3) buffer for approximately 2-3 hours at 120 V, followed by visualization under ultra violet light using the Kodak Digital Science Electrophoresis Documentation and Analysis System 120 (VilberLourmat, France).

Sanger Sequencing

PCR products were purified using the Wizard® SV Gel and PCR Clean-Up System (Promega, Madison, WI, USA). Sanger sequencing of PCR products were done at the Central Analytical Facility, Stellenbosch University. To determine the presence of polymorphisms in the gene region of interest, the CFZ resistant DNA sequences were aligned and compared to the *M. tuberculosis* K636 progenitor using BioEdit Sequence Alignment Editor (123).

3.4. Virtual Protein Visualisation

3.4.1. Protein Modelling

Wild type Rv0678 and the mutated protein which was identified in CFZ resistant clones were compared using protein modelling. The crystal structure of the wild type protein (PDB structure: 4NB5) was obtained from the Protein Data Bank (accession number: I6Y8F7) (124). The SWISS-MODEL Workspace, a homology-modelling server was used to model the mutated Rv0678 protein, using 4NB5.1.D as a template (125–127). Following the selection of 4NB5.1.D the “Target Prediction” was set to build a homo-tetramer. The model was predicted by SWISS-MODEL and a “pdb” file was obtained containing the predicted mutated Rv0678.

3.4.2. Visualisation Using Chimera

Chimera v1.9 (128) was used to visualise 4NB5 and the virtually modelled protein containing the non-synonymous SNP identified during WGS. Analysis of the 3D structures was performed on 4NB5 and the mutated Rv0678 to elucidate the influence that the non-synonymous SNP may have on the protein structure.

Chapter 4

Results

4.1. Clofazimine *in vitro* Mono-Resistant Mutant Generation

Nine clofazimine (CFZ) resistant colonies were initially obtained following the exposure of the pan-susceptible progenitor, *M. tuberculosis* K636, to 2.6 µg/ml CFZ. No growth was observed following exposure to 2.9 µg/ml CFZ. Subsequent sub-culturing in mycobacterial growth indicator tubes (MGIT) and re-exposure to CFZ showed that 5 of these isolates (CFZR2, CFZR6, CFZR7, CFZR8 and CFZR9) were resistant to the 0.5 µg/ml CFZ. These 5 isolates were characterised further.

4.2. Characterisation of the Clofazimine Mono-Drug Resistant Mutants

4.2.1. Growth Characteristics of Clones

The growth characteristics of CFZ resistant clones were identical to the susceptible progenitor K636 when cultured in 7H9+ADC at 37°C (Figure 4.1).

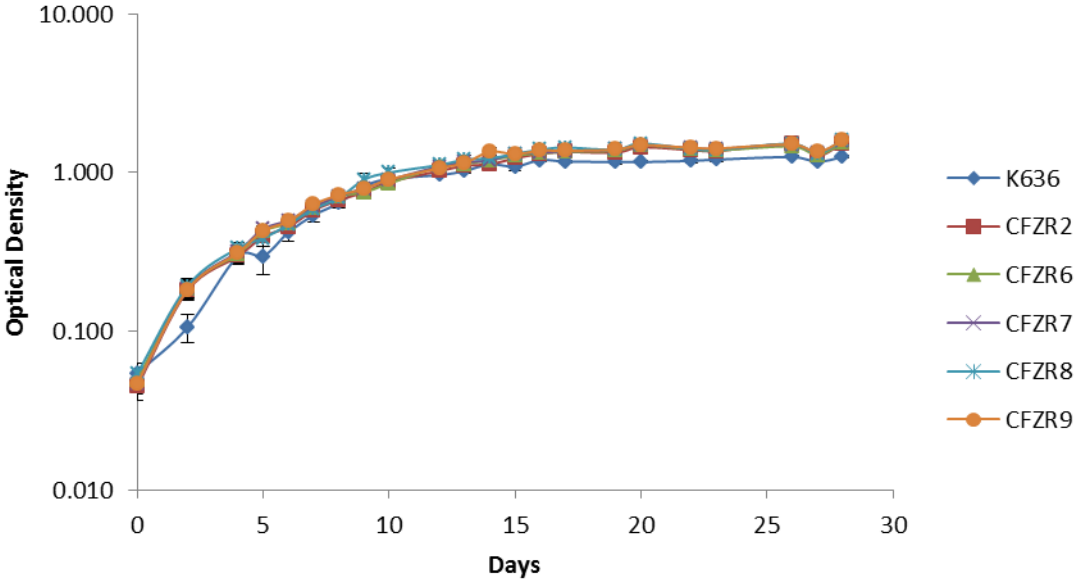

Figure 4.1: Growth curve comparing the progenitor *M. tuberculosis* strain (K636) and CFZ resistant clones (CFZR2, CFZR6, CFZR7, CFZR8 and CFZR9). The graph was plotted using the mean OD obtained from 3 biological, independent experiments. Error bars indicate the standard error around the mean of each value.

4.2.2. Colony and Cell Morphology

There was no difference in colony morphology observed between the progenitor *M. tuberculosis* strain (K636) and CFZ resistant clones.

Figure 4.2 shows the Ziehl-Neelsen (ZN) acid-fast staining of cells of K636 and the CFZ resistant clones CFZR2, CFZR6, CFZR7, CFZR8 and CFZR9. These microscopic views suggest that the cell morphology of the mutants was the same as the wild type strain, and that they were members of the genus Mycobacteria.

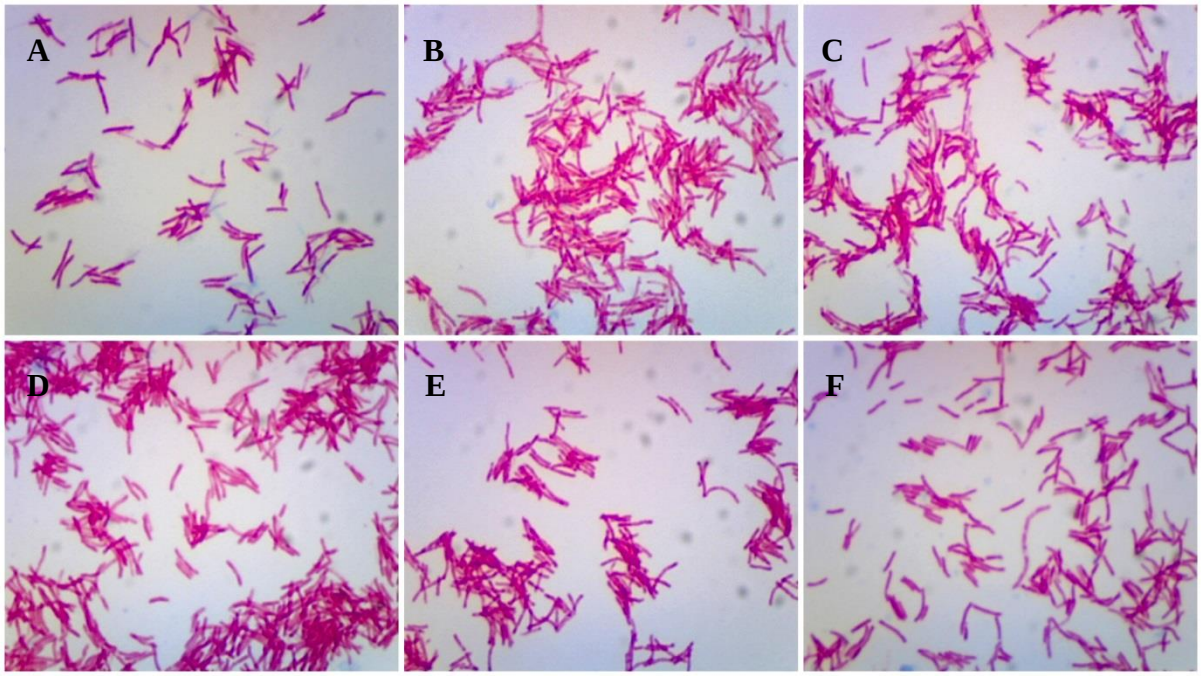

Figure 4.2: Images displaying Ziehl-Neelsen acid fast staining. (A) Progenitor *M. tuberculosis* strain (K636), (B) CFZR2, (C) CFZR6, (D) CFZR7, (E) CFZR8 and (F) CFZR9.

4.2.3. Strain Verification Using Spoligotyping

The spoligotype of the progenitor, K636, was identical to that of the CFZ resistance clones CFZR2, CFZR6, CFZR7, CFZR8 and CFZR9 (Table 4.1). This confirms that the CFZ resistant colonies were from the same genotype (Beijing) as K636.

Table 4.1: The spoligotyping results of the progenitor, K636, and the CFZ resistant mutants, CFZR2, CFZR6, CFZR7, CFZR8 and CFZR9.

Isolate	Spoligotype
K636	
CFZR2	
CFZR6	
CFZR7	
CFZR8	
CFZR9	

4.2.4. Minimum Inhibitory Concentration Determination in Liquid Media

The minimum inhibitory concentration (MIC) of the progenitor (K636) was <0.25 µg/ml. In comparison the MICs for the CFZ resistant clones CFZR2, CFZR6, CFZR8 and CFZR9 were >0.25 µg/ml and <0.5 µg/ml, while the MIC for CFZR7 was >0.50 µg/ml (Table 4.2).

Table 4.2: Minimum inhibitory concentration (MIC) of the progenitor (K636) and the CFZ resistant isolates (CFZR2, CFZR6, CFZR7, CFZR8 and CFZR9).

Isolate	CFZ MIC
K636	<0.25 µg/ml
CFZR2	>0.25 µg/ml
CFZR6	>0.25 µg/ml
CFZR7	>0.50 µg/ml
CFZR8	>0.25 µg/ml
CFZR9	>0.25 µg/ml

4.2.5. Minimum Inhibitory Concentration Determination Using Agar Dilution Method

Following exposure to 0.5 µg/ml CFZ the progenitor, K636, did not grow, while the CFZ resistant isolates grew in abundance. At a CFZ concentration of ≥1.0 µg/ml no growth was observed.

Table 4.3: The optical densities at which the clones were plated and the colony forming units of the clones at CFZ concentrations 0 µg/ml, 0.5 µg/ml, 1.0 µg/ml, 2.0 µg/ml, 2.5 µg/ml and 3.0 µg/ml.

Isolate	OD when plated	CFUs/ml at 0 µg/ml CFZ	CFUs/ml at 0.5 µg/ml CFZ	CFUs/ml at 1.0 µg/ml CFZ	CFUs/ml at 2.0 µg/ml CFZ	CFUs/ml at 2.5 µg/ml CFZ	CFUs/ml at 3.0 µg/ml CFZ
K636	0.477	155×10^6	0	0	0	0	0
CFZR2	0.600	615×10^6	>2500	0	0	0	0
CFZR6	0.685	763×10^6	>2500	0	0	0	0
CFZR7	0.654	730×10^6	>2500	0	0	0	0
CFZR8	0.563	722×10^6	>2500	0	0	0	0
CFZR9	0.699	830×10^6	>2500	0	0	0	0

4.3. Whole Genome Sequencing

Bioinformatic analyses using three alignment methods identified a total of 3 chromosomal variants uniquely present in all of the CFZ resistant clones described here (Table 4.4). Targeted sequencing validated the three identified variants. A g250a non-synonymous single nucleotide polymorphism (SNP) was identified in *Rv0678*, causing an amino acid (AA) change from Alanine to Threonine at codon 84.

A second mutation was observed in the *Rv2941* gene, where a 92 bp deletion was found which led to a premature stop codon. This premature stop resulted in the production of a

potential truncated protein of only 71 AA compared to the 580 AA encoded by the wild type gene.

The third mutation was the result of a 1 bp insertion in gene *Rv3696c*, resulting in the truncation of the GlpK glycerol kinase protein from 517 AA to 70 AA because of a premature stop codon.

Table 4.4: The variants identified during WGS of K636 and CFZR2 and CFZR7.

Gene	Protein	SNP/Insertion/Deletion	Effect on protein or gene
Rv0678	Regulator	g250a	Changed AA (A84T)
Rv2941	Fatty-acid-AMP-Ligase (FadD28)	92 bp deletion at 161	Premature stop codon in gene (Q71STOP)
Rv3696c	Glycerol Kinase (GlpK)	1 bp insertion at 573	Premature stop codon in gene (E252STOP)

4.4. Virtual Protein Visualisation

The mutation at codon 84 in *Rv0678* results in the replacement of the non-polar amino acid alanine with a polar amino acid, threonine, in the CFZ resistant clones (Figure 4.3). Threonine has two extra side chains which may influence the binding of the regulator, Rv0678, to DNA. Chimera v1.9 was used to visualise protein 4NB5 (124), representing the crystal structure of Rv0678, as well as the virtually modelled Rv0678 mutated protein (125–127). This enabled us to determine the effect of changed amino acids on the protein and how this change potentially could influence its interaction with its target.

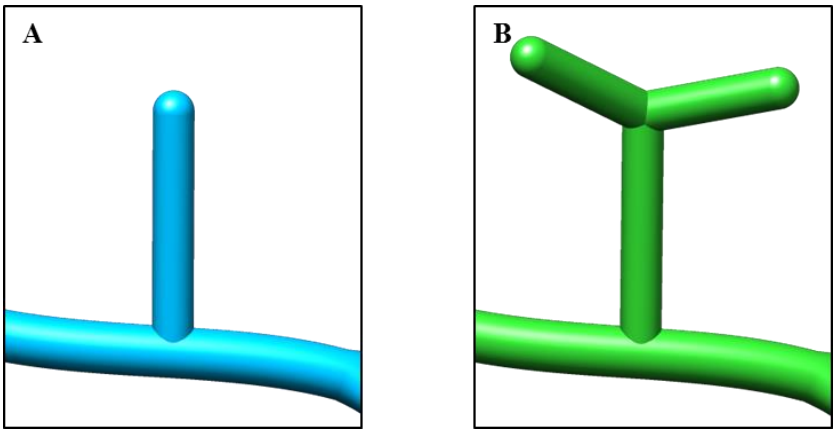

Figure 4.3: The (A) alanine, in the wild type, and (B) threonine, in the mutant, found at amino acid 84 in Rv0678.

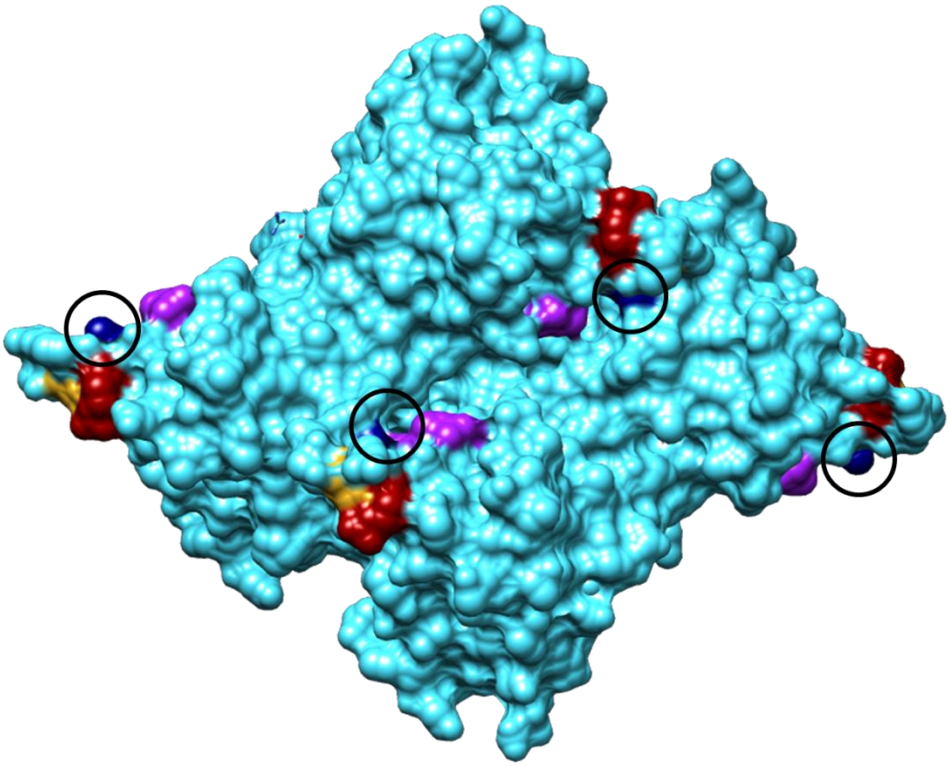

Figure 4.4: The surface of wild type Rv0678, showing DNA binding domains in purple (amino acid 82), yellow (amino acid 90) and red (amino acid 88), and amino acid 84 in dark blue.

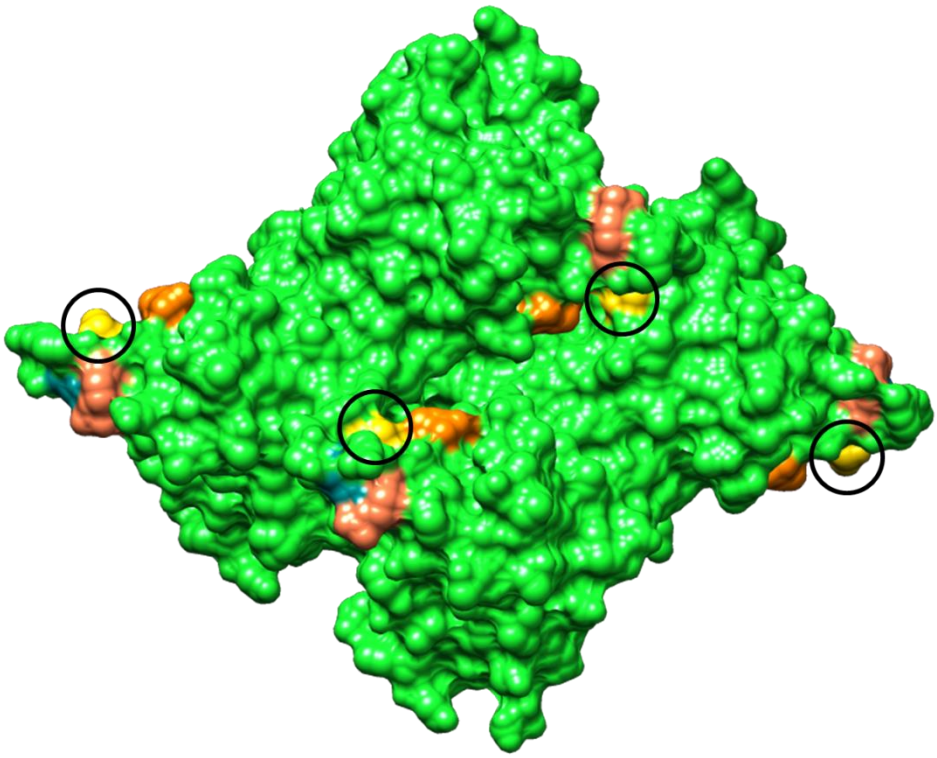

Figure 4.5: The codon 84 Rv0678 mutant, where the DNA binding domains are coloured coral (amino acid 82), blue (amino acid 88) and orange (amino acid 90), while amino acid 84 is coloured yellow.

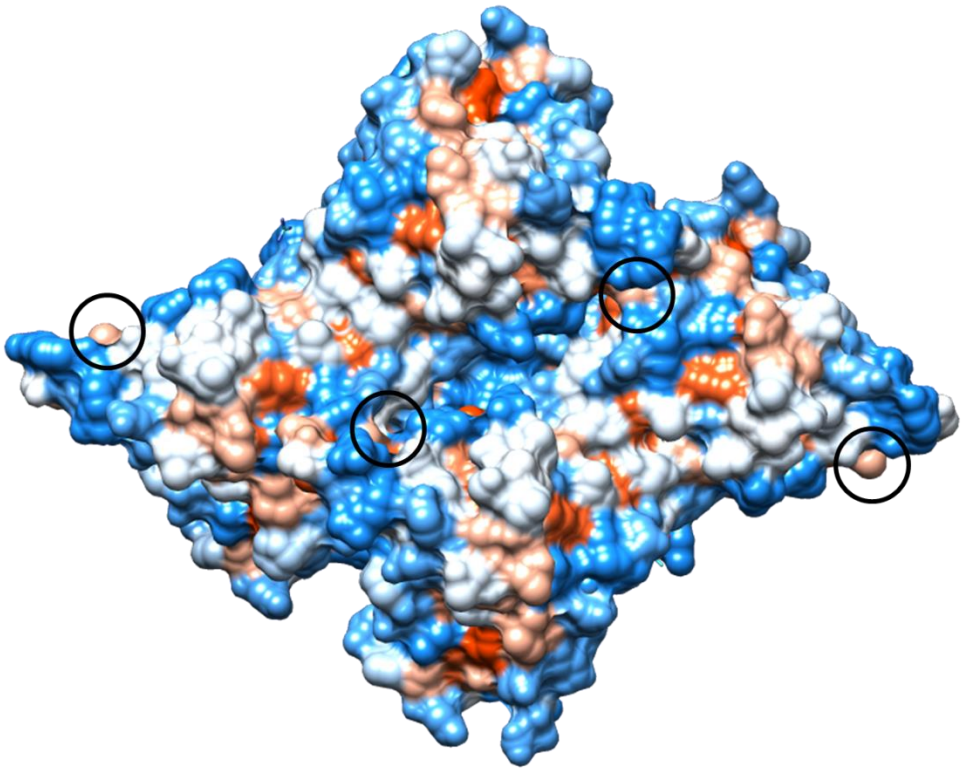

Figure 4.6: The surface of wild type Rv0678 showing the hydrophobicity of the protein, and all four of the amino acids at 84 in the homotetramer are circled.

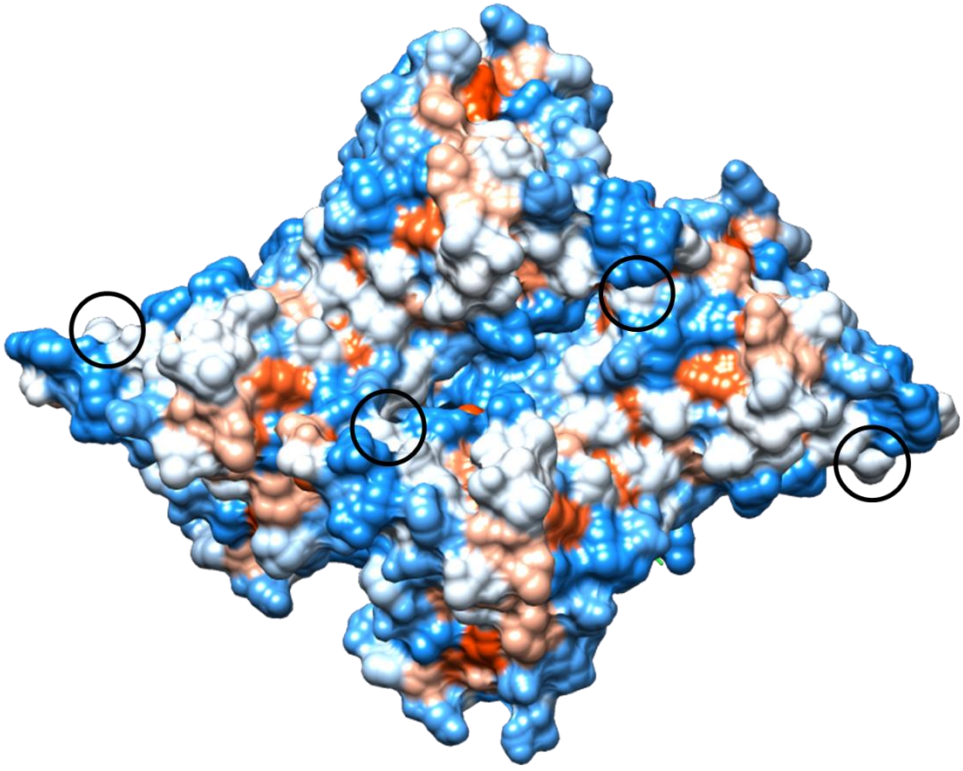

Figure 4.7: The surface of the mutated Rv0678, showing the hydrophobicity of the proteins, and all four of the 84th amino acids in the homotetramer are circled.

The A84T mutation at amino acid 84 is in the region of the DNA binding domain, which can be seen in Figure 4.4 and Figure 4.5. In Figure 4.6 and Figure 4.7 the change from hydrophobic to neutral caused by the mutation at amino acid 84 is displayed.

Chapter 5

Discussion

5.1. Mutations Identified in Clofazimine Resistant Isolates

During this study, a number of spontaneous clofazimine (CFZ) resistant mutants, with a 2 fold increase in minimum inhibitory concentration (MIC), were isolated from a clinical *M. tuberculosis* isolate following culture on media containing CFZ. These clones were all characterised by the same chromosomal mutations, namely a non-synonymous single nucleotide polymorphism (SNP) in *Rv0678*, a deletion in *Rv2941* and a single base-pair insertion in *Rv3696c*. Although mutations in *Rv0678* had been described previously, both in *in vitro* generated and clinical CFZ-resistant isolates (107, 108), all the mutations described in this study were novel and had not been previously described in the literature. These mutations occurred in genes involved in either the uptake or generation of specific nutrient components needed by *M. tuberculosis*. However, we could find no evidence to suggest that these mutations influenced the *in vitro* growth rate of the CFZ resistant mutants when compared to the wild type progenitor. This may be explained by the fact that the mutant clones were cultured on enriched media (7H9+ADC). Furthermore, there were no differences in the colony morphology of the progenitor and CFZ resistant mutant clones. This was expected since none of the genes with identified mutations has been reported to play a role in cell formation and division.

5.1.1. *Rv0678*

Although the mutation described in *Rv0678* was novel, earlier studies had identified mutations in *Rv0678*, a MarR-like regulator, in CFZ resistant isolates (107, 108). These studies observed that the S63R, S68G, R134STOP mutations, as well as frameshift mutations (caused by insertions at basepair 38 and 192) caused *in vitro* resistance to CFZ (107, 108). Sequencing of *in vivo* CFZ resistant isolates from patients also identified additional mutations W42R, T33A, A36V and frameshift mutations (caused by insertions at basepair 141 and 172 and a deletion at basepair 212) in *Rv0678* (107).

Not much is known about the role of the MarR-like regulator in *M. tuberculosis*. However, MarR regulators from other bacteria are known to control several important biological processes, including the production of virulence factors, oxidative stress responses and antimicrobial resistance (129). A search of the available literature revealed that mutations in

the *M. tuberculosis* MarR-like transcriptional regulator, encoded by *Rv0678*, were previously indicated in azole resistance in *M. tuberculosis* (130).

Mutations in *Rv0678* appeared to be linked to increased expression of an efflux pump which are encoded by genes situated directly upstream of *Rv0678* (108). Although we did not evaluate the expression of these genes in this study, it is plausible that the same phenomenon could be true for the CFZ resistant mutants described here. This suggests that the A84T mutation in *Rv0678*, identified in this study, causes upregulation of MmpS5-MmpL5 (mycobacterial membrane protein small 5 – mycobacterial membrane protein large 5), which is proposed to play a role in siderophore transport (131). A recent study found that the overexpression of MmpS5-MmpL5 leads to 2× increase in CFZ resistance (107) which corresponds to our observation that the CFZ MICs were increased by 2 fold. *Rv0678*, the MarR-like regulator contains a DNA binding domain targeting the DNA upstream of these genes. This binding interaction was confirmed using mobility gel-shift assays using DNA fragments complementary to the promoters of *mmpL5*, *mmpL2* and *mmpL4* operons (124). The gene encoding the regulator is also situated immediately downstream from this *mmpS5-mmpL5* operon in *M. tuberculosis* (Figure 5.1) (124).

Figure 5.1: The regulator gene, *Rv0678*, is located downstream of the *mmpS5-mmpL5* operon.

Rv0678 encodes a protein of 165 amino acids which forms a homodimer which in turn combines to form an asymmetric unit, consisting of two homodimers (124). According to Radhakrishnan *et al*. (2014) "three residues, Arg-84, Asp-90, and Arg-92, are located within the DNA-binding domain of the regulator and are probably important for protein DNA interactions" (124). Upon purification of the protein encoded by *Rv0678*, the fatty acid 2-stearoylglycerol was co-purified with the protein (124). Ligand screening indicated that this fatty acid molecule is buried completely within the interface of the dimer (124). This suggests that this fatty acid potentially plays a regulatory role in the mechanism of Rv0678. MarR type regulators have multiple substrates depending on the process being regulated (132), in one instance uric acid was found to bind to the MarR type regulator and thereby antagonize DNA-binding (133).

The mechanisms whereby MmpL proteins affect *M. tuberculosis* phenotypes are currently under investigation (134, 135). There are 13 MmpL proteins, in the *M. tuberculosis* genome, which are involved in efflux of multiple substrates. These MmpL proteins form part of the RND proteins which are involved in nodulation, cell division and resistance to antibiotics (135). MmpL proteins work together with MmpS as an efflux system. Evidence shows that these efflux systems are involved in lipid and fatty acid export (131, 135–139).

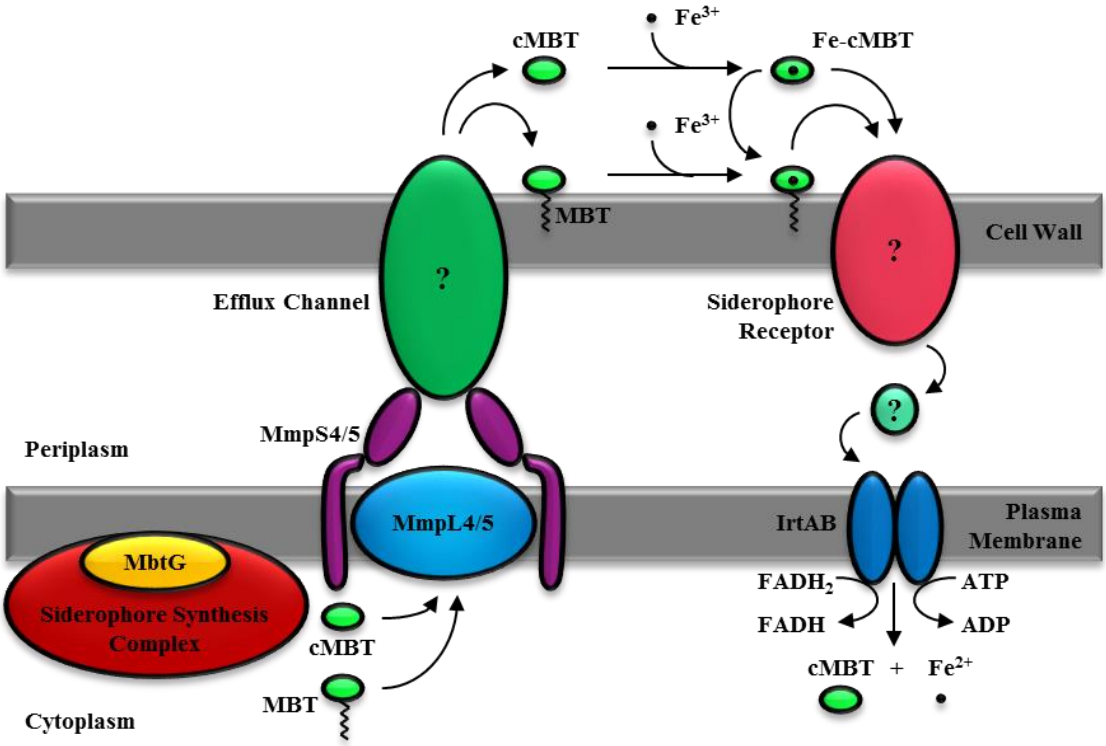

Figure 5.2: A schematic representation of the *M. tuberculosis* siderophore-mediated uptake of iron. Cytoplasmic synthases synthesise siderophores, which are suspected to be transported by the MmpS4-MmpL4 and MmpS5-MmpL5 export systems. The MmpS4 and MmpS5 proteins are situated in the plasma membrane, and coupled with their MmpL4 and MmpL5 counterparts respectively. A yet undiscovered cell wall protein would be required to export siderophores over the cell wall. Outside the cell siderophores bind to iron and requires another undiscovered cell wall protein to transport the complex back across the cell wall. IrtAB imports the ferric-siderophore from the periplasmic across the plasma membrane into the cytoplasm. Here the iron is available to the cell after releasing from the siderophore. (Adapted from (131))

It has been suggested that MmmS5-MmpL5 exports the siderophores; mycobactin and carboxymycobactin (131) (Figure 5.2). Siderophores bind to ferric iron (Fe^{3+}) outside the cell, transports it across the cell membrane and releases ferrous iron (Fe^{2+}) inside the cell (Figure 5.2). Fe^{2+} acts as an electron donor or acceptor in the electron transport chain (140). The electron transport chain drives adenosine triphosphate (ATP) synthesis, an essential

pathway for survival of the bacterium. It is thus plausible that upregulation of MmpS5-MmpL5 may lead to a higher level of iron within the cell. This could influence the levels of menaquinone in the cell, as it has been found that growing *M. tuberculosis* in an iron rich environment leads to a higher level of menaquinone than when grown in an iron-limited environment (141).

CFZ competes with menaquinone to be reduced by quinone oxidoreductase, a mycobacterial type II NADH oxidoreductase (NDH-2) (12). This NDH-2 has an essential role in the growth of *M. tuberculosis* because of this menaquinone reduction function. Other menaquinone producing resources within *M. tuberculosis* include mycobacterial type I NADH oxidoreductase (NDH-1) and succinate oxidoreductase (142).

Iron is an essential component for NDH-1 synthesis within the cell, since NDH-1 possess iron-sulphur cluster subunits (143). This suggests that the increase of iron within the cell, caused by the upregulation of MmpS5-MmpL5, could increase the amount of NDH-1 synthesised. An increase in the amount of NDH-1 present in the cell could lead to an increase in menaquinone reduction, counteracting the influence of CFZ.

Another explanation for increased CFZ resistance, caused by the upregulation of the MmpS5-MmpL5 efflux pump, could be the increase in efflux of the drug itself. Isoniazid resistance has been conferred through the overexpression of *M. tuberculosis* MmpL7 in *M. smegmatis* (144). Through the use of efflux pump inhibitors the MIC was decreased, confirming the influence of the efflux pump on isoniazid resistance (144).

Our observed lack of an influence on growth of the CFZ resistant mutants could be explained by the presence of iron in the 7H9+ADC, which is freely available in large quantities to the wild type, K636, *in vitro* (145, 146). However, studies with iron depleted media, or *in vivo* studies may display different results, since iron is not freely available to the organism, which could influence the growth.

5.1.2. Rv2941

The CFZ resistant mutants described here also contained a deletion in the *Rv2941* gene, which encodes a fatty-acid-AMP ligase (FadD28). The enzyme is involved in the production of the phthiocerol dimycocerosate (PDIM), a known *M. tuberculosis* virulence factor (147, 148). The 92 bp deletion identified in the gene causes a significant truncation of the protein. Not much is known about PDIMs and *M. tuberculosis* drug resistance, but a recent paper

showed elevated PDIM production in rifampicin resistant *M. tuberculosis* isolates (149). Conversely, diminished PDIM activity was shown to increase *M. tuberculosis* sensitivity to drugs and detergents, indicating an impaired cell and perhaps more permeable envelope protection (150).

Previous studies have not yet linked FadD28 to CFZ resistance. However, a recent study did find a mutation in *ppsC* in a CFZ resistant isolate with a mutation in Rv0678 (107). PpsC is involved in PDIM biosynthesis (150). There are three transcriptionally related units (Figure 5.3); (i) the first stretches from *fadD26* to *papA5*, (ii) the second consists of the *mas* gene, and (iii) the third include the open reading frame of *fadD28* and *mmpL7* (150). This suggests that the mutations in the genes responsible for PDIM synthesis may influence CFZ resistance. However, unfortunately no conclusions can be made about the role of FadD28 in CFZ resistance as no further studies have been done here to establish its role in these CFZ resistant clones.

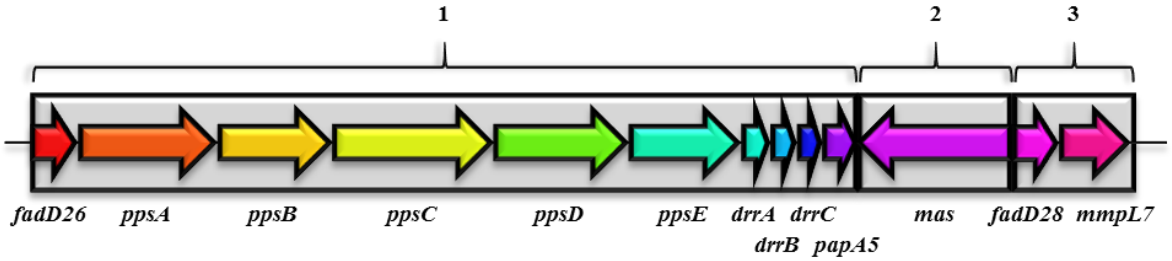

Figure 5.3: The transcriptional related units 1-3; unit 1 contains *ppsC* and unit 3 contains *fadD28*. (Adapted from (25))

The truncation of FadD28 did not influence the growth of the organism *in vitro*. This is in line with observations that *in vitro* growth of *M. tuberculosis* does not require PDIM virulence factors (151). Conversely other studies have found that when *M. tuberculosis* H37Rv loses PDIM synthesis (when grown *in vitro* for extended periods of time) this leads to attenuated growth *in vivo* (151, 152).

5.1.3. *Rv3696c*

The last gene that was found to be mutated in these CFZ resistant mutants was *Rv3696c*, encoding glycerol kinase (GlpK). This enzyme converts glycerol to glycerol-3-phosphate, which enters the central carbon metabolism (153). Glycerol-3-phosphate production in *M. tuberculosis* "is essential for membrane and fatty acid metabolism involving fatty-acyl

glycerol phosphates and interconversions between CDP-diacyl-glycerol and phosphatidyl-glycerol phosphates" (154). However, it is not essential for growth *in vivo* in mice (61).

The truncation of GlpK, in this study, is the result of a 1 bp insertion. Mutations in GlpK have not previously been linked with resistance to CFZ. This mutation also does not seem to influence *in vitro* growth. However, previous studies using either transposon site hybridisation or knockout mutants of GlpK showed a negative effect on growth on glucose enriched media (45, 155). The knockout mutant of GlpK failed to grow on glycerol minimal media (45). Another study where a *M. bovis glpK* mutant was generated the protein was truncated due to a frameshift. This mutant could not survive on glycerol media, pyruvate had to be added before growth was observed (156). GlpK is needed *in vivo* to metabolize glycerol, the carbon source for the organism within the host. Since glucose is present in 7H9+ADC, GlpK may not be necessary for *in vitro* growth.

5.2. Clinical Consequences of Clofazimine Resistance

CFZ currently is one of the drugs reserved as a last resort in tuberculosis (TB) therapy. Current clinical trials are also looking at its interaction with newer available drugs, in an effort to find more effective therapies for drug resistant TB. In leprosy, where this drug is currently in use, drug resistance is rare (10). This may be explained by the absence of *Rv0678* and *mmpS5-mmpL5* in *M. leprae* (157–163).

Older literature suggested that CFZ does not induce resistance in *M. tuberculosis*, but recent studies clearly demonstrated the development of CFZ resistant both *in vitro* and in patients (83). Not only does exposure to CFZ result in resistance, but exposure to one of the new anti-TB drugs also generates CFZ resistance. The observed cross-resistance between bedaquiline (BDQ) and CFZ may influence treatment regimens, particularly if alternative therapeutic options are not available. Such induced cross resistance was recently described in a Tibetan man admitted with multiple drug-resistant TB (MDR-TB) in January 2011 (109). The patient was initially treated with a combination of ethambutol (EMB), para-aminosalicylic acid (PAS), cycloserine (CYC) and capreomycin (CAP) (109). From September 2011 to February 2012 the patient also received BDQ on compassionate grounds. Therapy continued until March 2013, resulting in culture conversion in October 2011 (109). When the patient was re-admitted in August 2013, therapy was continued with EMB, PAS, CYC, CAP, CFZ and amikacin (109).

Drug susceptibility tests (DSTs) revealed that the 2013 relapse isolate had the same drug resistance pattern as the initial MDR-TB isolate, except that the latest isolate was also resistant to CFZ. Analysis of *Rv0678*, explained the cause of CFZ resistance by Hartkroon *et al*. (2014) revealed that the 2011 isolate displayed a wild-type sequence, while the CFZ resistant isolate had a non-synonymous mutation at the second base pair, causing a methionine to alanine codon change (109). The observed mutation (M1A) caused the loss of Rv0678 expression and was regarded as the most probable cause of CFZ resistance (109).

During another study clinical isolates with an increased BDQ post-baseline MIC were selected (107). The *Rv0678* gene of these isolates were sequenced, and revealed mutations in the gene and following MIC testing the isolates displayed CFZ cross-resistance (107).

This observation has important consequences for drug development. Currently the TB Alliance has three regimens in their pipeline where BDQ and CFZ are both in the same regimen. The cross-resistance which has recently been identified between BDQ and CFZ will render these regimens potentially inadequate (108, 109). This observation implies that BDQ therapy, for an unknown reason, could promote the development of mutations in Rv0678, rendering CFZ useless as a back-up therapy regimen. Although the reason for the mutational evolution is unclear, it was observed by others that exposure to drugs which influence energy metabolism genes (BDQ, azoles and CFZ), all result in mutations in *Rv0678* (108, 109, 130). These mutations inactivate the DNA binding protein and its transcriptional regulatory activity, ultimately leading to increased expression of genes involved in siderophore transport across the cell membrane (108, 131). A further concern is that upregulation of these genes does not have a growth defect *in vitro* or in mice (107), suggesting the absence of a fitness cost associated with the emergence of CFZ resistance.

5.3. Future Studies

In order to evaluate the role of the different mutations on CFZ resistance, each gene described in this study should be evaluated independently. Such studies should include the generation of single mutants generated by targeting the individual genes. The role of *Rv0678* has already been established in CFZ resistance from clinical isolates. However, the effect on the fitness of the bacterium *in vivo* should be explored. Such studies would help to establish if the lack of a fitness deficit might aid the spread of CFZ resistant drug isolates between people. In the future, a CFZ resistant mutant containing a non-synonymous mutation in Rv0678 should be

grown in iron depleted media. If the CFZ resistant isolate is less resistant to CFZ it validates the role of iron in CFZ resistance described in Chapter 5.1.1.

Another way to further investigate the influence of each gene is the construction of single gene knockouts. Only after knocking out individual genes can the full extent of the influence that the gene has on CFZ resistance be determined.

Chapter 6

Conclusion

Identifying the molecular mechanisms of CFZ resistance are essential for enabling the development of proper diagnostic screens in patients who have multidrug resistant tuberculosis and require treatment with CFZ.

During this study three novel, non-synonymous mutations were identified in CFZ resistant clones. Two of these resulted in premature stop codons in the respective genes, namely a 92 bp deletion in *Rv2941* and a 1 bp insertion in *Rv3696c*. The third mutation was located in *Rv0678*, a gene previously associated with CFZ resistance. However, the mutation we identified in this study had not been previously described, namely A84T (107, 108).

Although the mutation in *Rv0678* is novel, we hypothesised that this mutation was the most probable cause of CFZ resistance in this clone. However confirmation studies need to be done to verify the role of this novel mutation. We hypothesise that this mutation, like previously described *Rv0678* mutations leads to upregulation of a specific efflux pump associated with siderophore transport in *M. tuberculosis*. More studies also need to be done to establish how this upregulation leads to CFZ resistance.

The remaining two mutations have not been associated with CFZ resistance in other studies. However, the gene product of *Rv2941*, a fatty-acid-AMP ligase (FadD28), had been associated with the product of another gene, *ppsC*, of which a mutation had been described in a clinical CFZ resistant isolate which also contained an insertion in Rv0678 (107). Both FadD28 and PpsC are involved in phthiocerol dimycocerosates (PDIM) biosynthesis, which is known to affect the sensitivity of *M. tuberculosis* to antibacterial drugs. *Rv2941* also has strong associations with other cell-wall associated proteins, thus it can be hypothesised that CFZ sensitivity potentially could be affected by the cell wall integrity of *M. tuberculosis*. However, studies need to be done to assess an association between PDIM biosynthesis and sensitivity to CFZ before conclusions can be drawn. The third mutation, a 1 bp insertion in *Rv3696c*, is not suspected to play a role in CFZ resistance, but this needs to be confirmed.

In summary, we identified a novel mutation in a *M. tuberculosis* gene with a known role of resistance to CFZ. This work thus supports the previously described role of the *Rv0678* gene product in CFZ resistance and suggests that this gene is a strong candidate for clinical

diagnostic screens to identify CFZ resistance in *M. tuberculosis* clinical isolates. The roles of the additional novel mutants in modulating CFZ resistance requires further investigation.

Reference List

1. Ford CB, Lin PL, Chase MR, Shah RR, Iartchouk O, Galagan J, Mohaideen N, Ioerger TR, Sacchettini JC, Lipsitch M, Flynn JL, Fortune SM. 2011. Use of whole genome sequencing to estimate the mutation rate of *Mycobacterium tuberculosis* during latent infection. Nat. Genet. 43:482–486.
2. World Health Organization. Global tuberculosis report 2013. WHO.
3. Addington WW. 1979. Patient compliance: the most serious remaining problem in the control of tuberculosis in the United States. Chest 76:741–743.
4. Fox W. 1983. Compliance of patients and physicians: experience and lessons from tuberculosis-I. Br. Med. J. Clin. Res. Ed 287:33–35.
5. M'Imunya JM, Kredo T, Volmink J. 1996. Patient education and counselling for promoting adherence to treatment for tuberculosis. Cochrane Database of Systematic Reviews. John Wiley & Sons, Ltd.
6. Burian J, Ramón-García S, Howes CG, Thompson CJ. 2012. WhiB7, a transcriptional activator that coordinates physiology with intrinsic drug resistance in *Mycobacterium tuberculosis*. Expert Rev. Anti Infect. Ther. 10:1037–1047.
7. Dey T, Brigden G, Cox H, Shubber Z, Cooke G, Ford N. 2013. Outcomes of clofazimine for the treatment of drug-resistant tuberculosis: a systematic review and meta-analysis. J. Antimicrob. Chemother. 68:284–293.
8. Lienhardt C, Raviglione M, Spigelman M, Hafner R, Jaramillo E, Hoelscher M, Zumla A, Gheuens J. 2012. New drugs for the treatment of tuberculosis: needs, challenges, promise, and prospects for the future. J. Infect. Dis. 205 Suppl 2:S241–249.
9. Zhang D, Lu Y, Liu K, Liu B, Wang J, Zhang G, Zhang H, Liu Y, Wang B, Zheng M, Fu L, Hou Y, Gong N, Lv Y, Li C, Cooper CB, Upton AM, Yin D, Ma Z, Huang H. 2012. Identification of less lipophilic riminophenazine derivatives for the treatment of drug-resistant tuberculosis. J. Med. Chem. 55:8409–8417.
10. Matsuoka M. 2010. Drug resistance in leprosy. Jpn. J. Infect. Dis. 63:1–7.
11. Mitnick C, Horsburgh CR Jr. 2010. Encouraging news for multidrug-resistant tuberculosis treatment. Am. J. Respir. Crit. Care Med. 182:1337–1338.
12. Yano T, Kassovska-Bratinova S, Teh JS, Winkler J, Sullivan K, Isaacs A, Schechter NM, Rubin H. 2011. Reduction of clofazimine by mycobacterial type 2 NADH:quinone oxidoreductase: a pathway for the generation of bactericidal levels of reactive oxygen species. J. Biol. Chem. 286:10276–10287.

13. Long ER. 1948. Tuberculosis in Germany. Proc. Natl. Acad. Sci. U. S. A. 34:271–277.
14. Williams RL, Medalie JH, Zyzanski SJ, Flocke SA, Yaari S, Goldbourt U. 1993. Long term mortality of NAZI concentration camp survivors. J. Clin. Epidemiol. 46:573–575.
15. Schatz A, Bugle E, Waksman SA. 1944. Streptomycin, a substance exhibiting antibiotic activity against gram-positive and gram-negative bacteria. Exp. Biol. Med. 55:66–69.
16. Ozcaglar C, Shabbeer A, Vandenberg SL, Yener B, Bennett KP. 2012. Epidemiological models of *Mycobacterium tuberculosis* complex infections. Math. Biosci. 236:77–96.
17. Vynnycky E, Fine PE. 1997. The natural history of tuberculosis: the implications of age-dependent risks of disease and the role of reinfection. Epidemiol. Infect. 119:183–201.
18. Marshall G, Blacklock JWS, Cameron C, Capon NB, Cruickshank R, Gaddum JH, Heaf FRG, Bradford Hill A, Houghton LE, Clifford Hoyle J, Raistrick H, Scadding JG, Tytler WH, Wilson GS, D'Arcy Hart P. 1948. Streptomycin Treatment of Pulmonary Tuberculosis. Br. Med. J. 2:769–782.
19. Graessle OE, Pietrowski JJ. 1949. The in vitro efect of para-aminosalicylic acid (PAS) in preventing acquired resistance to streptomycin by *Mycobacterium tuberculosis*. J. Bacteriol. 57:459–464.
20. Grunberg E, Leiwant B, D'Ascensio IL, Schintzer RJ. 1952. On the lasting protective effect of hydrazine derivatives of isonicotinic acid in the experimental tuberculosis infection of mice. Dis. Chest 21:369–377.
21. Kushner S, Dalalian H, Sanjurjo JL, Bach FL, Safir SR, Smith VK, Williams JH. 1952. Experimental chemotherapy of tuberculosis. II. The synthesis of pyrazinamides and related compounds. J. Am. Chem. Soc. 74:3617–3621.
22. Nguyen L, Thompson CJ. 2006. Foundations of antibiotic resistance in bacterial physiology: the mycobacterial paradigm. Trends Microbiol. 14:304–312.
23. Raviglione MC, Dye C, Schmidt S, Kochi A. 1997. Assessment of worldwide tuberculosis control. The Lancet 350:624–629.
24. Johnson R, Streicher EM, Louw GE, Warren RM, van Helden PD, Victor TC. 2006. Drug resistance in *Mycobacterium tuberculosis*. Curr. Issues Mol. Biol. 8:97–111.
25. Wong SY, Lee JS, Kwak HK, Via LE, Boshoff HIM, Barry CE. 2011. Mutations in *gidB* confer low-level streptomycin resistance in *Mycobacterium tuberculosis*. Antimicrob. Agents Chemother. 55:2515–2522.

26. Wang X-D, Gu J, Wang T, Bi L-J, Zhang Z-P, Cui Z-Q, Wei H-P, Deng J-Y, Zhang X-E. 2011. Comparative analysis of mycobacterial NADH pyrophosphatase isoforms reveals a novel mechanism for isoniazid and ethionamide inactivation. Mol. Microbiol. 82:1375–1391.
27. Nusrath Unissa A, Selvakumar N, Narayanan S, Narayanan PR. 2008. Molecular analysis of isoniazid-resistant clinical isolates of *Mycobacterium tuberculosis* from India. Int. J. Antimicrob. Agents 31:71–75.
28. Shi W, Zhang X, Jiang X, Yuan H, Lee JS, Barry CE, Wang H, Zhang W, Zhang Y. 2011. Pyrazinamide inhibits trans-translation in *Mycobacterium tuberculosis*. Science 333:1630–1632.
29. Zhang Y. 2005. The magic bullets and tuberculosis drug targets. Annu. Rev. Pharmacol. Toxicol. 45:529–564.
30. Srivastava S, Musuka S, Sherman C, Meek C, Leff R, Gumbo T. 2010. Efflux-pump derived multiple drug resistance to ethambutol monotherapy in *Mycobacterium tuberculosis* and ethambutol pharmacokinetics-pharmacodynamics. J. Infect. Dis. 201:1225–1231.
31. Kalokhe AS, Shafiq M, Lee JC, Ray SM, Wang YF, Metchock B, Anderson AM, Ly T. Nguyen M. 2013. Multidrug-resistant tuberculosis drug susceptibility and molecular diagnostic testing. Am. J. Med. Sci. 345:143–148.
32. Bruning JB, Murillo AC, Chacon O, Barletta RG, Sacchettini JC. 2011. Structure of the *Mycobacterium tuberculosis* d-alanine:d-alanine ligase, a target of the antituberculosis drug d-cycloserine. Antimicrob. Agents Chemother. 55:291–301.
33. Rastogi N, David HL. 1993. Mode of action of antituberculous drugs and mechanisms of drug resistance in *Mycobacterium tuberculosis*. Res. Microbiol. 144:133–143.
34. Winder FG, Collins PB, Whelan D. 1971. Effects of ethionamide and isoxyl on mycolic acid synthesis in *Mycobacterium tuberculosis* BCG. J. Gen. Microbiol. 66:379–380.
35. Drlica K. 1999. Mechanism of fluoroquinolone action. Curr. Opin. Microbiol. 2:504–508.
36. Palomino JC, Martin A. 2013. Is repositioning of drugs a viable alternative in the treatment of tuberculosis? J. Antimicrob. Chemother. 68:275–283.
37. Groll AV, Martin A, Jureen P, Hoffner S, Vandamme P, Portaels F, Palomino JC, Silva PA da. 2009. Fluoroquinolone resistance in *Mycobacterium tuberculosis* and mutations in *gyrA* and *gyrB*. Antimicrob. Agents Chemother. 53:4498–4500.

38. 2006. World Health Organization: The Stop TB Strategy. WHO.
39. Migliori GB, Dheda K, Centis R, Mwaba P, Bates M, O'Grady J, Hoelscher M, Zumla A. 2010. Review of multidrug-resistant and extensively drug-resistant TB: global perspectives with a focus on sub-Saharan Africa. Trop. Med. Int. Health 15:1052–1066.
40. Zumla A, Nahid P, Cole ST. 2013. Advances in the development of new tuberculosis drugs and treatment regimens. Nat. Rev. Drug Discov. 12:388–404.
41. Griffin JE, Gawronski JD, DeJesus MA, Ioerger TR, Akerley BJ, Sassetti CM. 2011. High-resolution phenotypic profiling defines genes essential for mycobacterial growth and cholesterol catabolism. PLoS Pathog 7:e1002251.
42. Sassetti CM, Boyd DH, Rubin EJ. 2001. Comprehensive identification of conditionally essential genes in mycobacteria. Proc. Natl. Acad. Sci. 98:12712–12717.
43. Warner DF, Mizrahi V. 2012. Approaches to target identification and validation for tuberculosis drug discovery: A University of Cape Town perspective. SAMJ South Afr. Med. J. 102:457–461.
44. Rhee KY, Carvalho LPS de, Bryk R, Ehrt S, Marrero J, Park SW, Schnappinger D, Venugopal A, Nathan C. 2011. Central carbon metabolism in *Mycobacterium tuberculosis*: an unexpected frontier. Trends Microbiol. 19:307–314.
45. Beste DJV, McFadden J. 2010. System-level strategies for studying the metabolism of *Mycobacterium tuberculosis*. Mol. Biosyst. 6:2363–2372.
46. De Carvalho LPS, Fischer SM, Marrero J, Nathan C, Ehrt S, Rhee KY. 2010. Metabolomics of *Mycobacterium tuberculosis* reveals compartmentalized co-catabolism of carbon substrates. Chem. Biol. 17:1122–1131.
47. Kinnings SL, Liu N, Buchmeier N, Tonge PJ, Xie L, Bourne PE. 2009. Drug discovery using chemical systems biology: repositioning the safe medicine comtan to treat multi-drug and extensively drug resistant tuberculosis. PLoS Comput Biol 5:e1000423.
48. Russell DG, Barry CE, Flynn JL. 2010. Tuberculosis: what we don't know can, and does, hurt us. Science 328:852–856.
49. Lenaerts AJ, Gruppo V, Marietta KS, Johnson CM, Driscoll DK, Tompkins NM, Rose JD, Reynolds RC, Orme IM. 2005. Preclinical testing of the nitroimidazopyran PA-824 for activity against *Mycobacterium tuberculosis* in a series of *in vitro* and *in vivo* models. Antimicrob. Agents Chemother. 49:2294–2301.
50. Zhou H, Wang Y, Wang W, Jia J, Li Y, Wang Q, Wu Y, Tang J. 2009. Generation of monoclonal antibodies against highly conserved antigens. PLoS ONE 4:e6087.

51. Singh V, Chandra D, Srivastava BS, Srivastava R. 2011. Downregulation of *Rv0189c*, encoding a dihydroxyacid dehydratase, affects growth of *Mycobacterium tuberculosis* in vitro and in mice. Microbiology 157:38–46.
52. Via LE, Lin PL, Ray SM, Carrillo J, Allen SS, Eum SY, Taylor K, Klein E, Manjunatha U, Gonzales J, Lee EG, Park SK, Raleigh JA, Cho SN, McMurray DN, Flynn JL, Barry CE. 2008. Tuberculous granulomas are hypoxic in guinea pigs, rabbits, and nonhuman primates. Infect. Immun. 76:2333–2340.
53. Hoff DR, Caraway ML, Brooks EJ, Driver ER, Ryan GJ, Peloquin CA, Orme IM, Basaraba RJ, Lenaerts AJ. 2008. Metronidazole lacks antibacterial activity in guinea pigs infected with *Mycobacterium tuberculosis*. Antimicrob. Agents Chemother. 52:4137–4140.
54. Brooks JV, Furney SK, Orme IM. 1999. Metronidazole therapy in mice infected with tuberculosis. Antimicrob. Agents Chemother. 43:1285–1288.
55. Lin PL, Dartois V, Johnston PJ, Janssen C, Via L, Goodwin MB, Klein E, Barry CE, Flynn JL. 2012. Metronidazole prevents reactivation of latent *Mycobacterium tuberculosis* infection in macaques. Proc. Natl. Acad. Sci. 109:14188–14193.
56. Hughes J, Rees S, Kalindjian S, Philpott K. 2011. Principles of early drug discovery. Br. J. Pharmacol. 162:1239–1249.
57. Bologa CG, Ursu O, Oprea TI, Melançon III CE, Tegos GP. 2013. Emerging trends in the discovery of natural product antibacterials. Curr. Opin. Pharmacol. 13:678–687.
58. Fleming A. 1929. On the antibacterial action of cultures of a *Penicillium*, with special reference to their use in the isolation of *B. influenzae*. Br. J. Exp. Pathol. 10:226–236.
59. Newman DJ, Cragg GM. 2012. Natural products as sources of new drugs over the 30 years from 1981 to 2010. J. Nat. Prod. 75:311–335.
60. De Bruijn I, de Kock MJD, de Waard P, van Beek TA, Raaijmakers JM. 2008. Massetolide A biosynthesis in *Pseudomonas fluorescens*. J. Bacteriol. 190:2777–2789.
61. Pethe K, Sequeira PC, Agarwalla S, Rhee K, Kuhen K, Phong WY, Patel V, Beer D, Walker JR, Duraiswamy J, Jiricek J, Keller TH, Chatterjee A, Tan MP, Ujjini M, Rao SPS, Camacho L, Bifani P, Mak PA, Ma I, Barnes SW, Chen Z, Plouffe D, Thayalan P, Ng SH, Au M, Lee BH, Tan BH, Ravindran S, Nanjundappa M, Lin X, Goh A, Lakshminarayana SB, Shoen C, Cynamon M, Kreiswirth B, Dartois V, Peters EC, Glynne R, Brenner S, Dick T. 2010. A chemical genetic screen in *Mycobacterium tuberculosis* identifies carbon-source-dependent growth inhibitors devoid of *in vivo* efficacy. Nat. Commun. 1:57.

62. Muñoz-Elías EJ, McKinney JD. 2005. *Mycobacterium tuberculosis* isocitrate lyases 1 and 2 are jointly required for *in vivo* growth and virulence. Nat. Med. 11:638–644.

63. Andries K, Verhasselt P, Guillemont J, Göhlmann HWH, Neefs J-M, Winkler H, Gestel JV, Timmerman P, Zhu M, Lee E, Williams P, Chaffoy D de, Huitric E, Hoffner S, Cambau E, Truffot-Pernot C, Lounis N, Jarlier V. 2005. A diarylquinoline drug active on the ATP synthase of *Mycobacterium tuberculosis*. Science 307:223–227.

64. Mayr LM, Bojanic D. 2009. Novel trends in high-throughput screening. Curr. Opin. Pharmacol. 9:580–588.

65. Reynolds RC, Ananthan S, Faaleolea E, Hobrath JV, Kwong CD, Maddox C, Rasmussen L, Sosa MI, Thammasuvimol E, White EL, Zhang W, Secrist III JA. 2012. High throughput screening of a library based on kinase inhibitor scaffolds against *Mycobacterium tuberculosis* H37Rv. Tuberculosis 92:72–83.

66. Stanley SA, Grant SS, Kawate T, Iwase N, Shimizu M, Wivagg C, Silvis M, Kazyanskaya E, Aquadro J, Golas A, Fitzgerald M, Dai H, Zhang L, Hung DT. 2012. Identification of novel inhibitors of *M. tuberculosis* growth using whole cell based high-throughput screening. ACS Chem. Biol. 7:1377–1384.

67. Giuliano KA, DeBiasio RL, Dunlay RT, Gough A, Volosky JM, Zock J, Pavlakis GN, Taylor DL. 1997. High-content screening: a new approach to easing key bottlenecks in the drug discovery process. J. Biomol. Screen. 2:249–259.

68. Christophe T, Jackson M, Jeon HK, Fenistein D, Contreras-Dominguez M, Kim J, Genovesio A, Carralot J-P, Ewann F, Kim EH, Lee SY, Kang S, Seo MJ, Park EJ, Škovierová H, Pham H, Riccardi G, Nam JY, Marsollier L, Kempf M, Joly-Guillou M-L, Oh T, Shin WK, No Z, Nehrbass U, Brosch R, Cole ST, Brodin P. 2009. High content screening identifies decaprenyl-phosphoribose 2′ epimerase as a target for intracellular antimycobacterial inhibitors. PLoS Pathog 5:e1000645.

69. Sacchettini JC, Rubin EJ, Freundlich JS. 2008. Drugs versus bugs: in pursuit of the persistent predator *Mycobacterium tuberculosis*. Nat. Rev. Microbiol. 6:41–52.

70. Alland D, Steyn AJ, Weisbrod T, Aldrich K, Jacobs WR. 2000. Characterization of the *Mycobacterium tuberculosis iniBAC* promoter, a promoter that responds to cell wall biosynthesis inhibition. J. Bacteriol. 182:1802–1811.

71. Kanebratt KP, Andersson TB. 2008. Evaluation of HepaRG cells as an *in vitro* model for human drug metabolism studies. Drug Metab. Dispos. 36:1444–1452.

72. Kolb HC, Finn MG, Sharpless KB. 2001. Click chemistry: diverse chemical function from a few good reactions. Angew. Chem. Int. Ed. 40:2004–2021.
73. Labadie GR, Iglesia A de la, Morbidoni HR. 2011. Targeting tuberculosis through a small focused library of 1,2,3-triazoles. Mol. Divers. 15:1017–1024.
74. Zartler ER, Shapiro MJ. 2005. Fragonomics: fragment-based drug discovery. Curr. Opin. Chem. Biol. 9:366–370.
75. Perryman AL, Zhang Q, Soutter HH, Rosenfeld R, McRee DE, Olson AJ, Elder JE, David Stout C. 2010. Fragment-based screen against HIV protease. Chem. Biol. Drug Des. 75:257–268.
76. Oprea TI, Matter H. 2004. Integrating virtual screening in lead discovery. Curr. Opin. Chem. Biol. 8:349–358.
77. Cho Y, Ioerger TR, Sacchettini JC. 2008. Discovery of novel nitrobenzothiazole inhibitors for *Mycobacterium tuberculosis* ATP phosphoribosyl transferase (HisG) through virtual screening. J. Med. Chem. 51:5984–5992.
78. Pellecchia M, Sem DS, Wüthrich K. 2002. NMR in drug discovery. Nat. Rev. Drug Discov. 1:211.
79. Osman K, Evangelopoulos D, Basavannacharya C, Gupta A, McHugh TD, Bhakta S, Gibbons S. 2012. An antibacterial from *Hypericum acmosepalum* inhibits ATP-dependent MurE ligase from *Mycobacterium tuberculosis*. Int. J. Antimicrob. Agents 39:124–129.
80. Sova M, Kovač A, Turk S, Hrast M, Blanot D, Gobec S. 2009. Phosphorylated hydroxyethylamines as novel inhibitors of the bacterial cell wall biosynthesis enzymes MurC to MurF. Bioorganic Chem. 37:217–222.
81. Jagannath C, Reddy MV, Kailasam S, O'Sullivan JF, Gangadharam PR. 1995. Chemotherapeutic activity of clofazimine and its analogues against Mycobacterium tuberculosis. *in vitro*, intracellular, and *in vivo* studies. Am. J. Respir. Crit. Care Med. 151:1083–1086.
82. Venkatesan K, Deo N, Gupta UD. 2007. Tissue distribution and deposition of clofazimine in mice following oral administration with or without isoniazid. Arzneimittelforschung. 57:472–474.
83. Reddy VM, O'Sullivan JF, Gangadharam PR. 1999. Antimycobacterial activities of riminophenazines. J. Antimicrob. Chemother. 43:615–623.
84. Brodin P, Christophe T. 2011. High-content screening in infectious diseases. Curr. Opin. Chem. Biol. 15:534–539.

85. Keserű GM, Makara GM. 2006. Hit discovery and hit-to-lead approaches. Drug Discov. Today 11:741–748.

86. Baxter A, Brough S, Cooper A, Floettmann E, Foster S, Harding C, Kettle J, McInally T, Martin C, Mobbs M, Needham M, Newham P, Paine S, St-Gallay S, Salter S, Unitt J, Xue Y. 2004. Hit-to-lead studies: the discovery of potent, orally active, thiophenecarboxamide IKK-2 inhibitors. Bioorg. Med. Chem. Lett. 14:2817–2822.

87. Baxter A, Bent J, Bowers K, Braddock M, Brough S, Fagura M, Lawson M, McInally T, Mortimore M, Robertson M, Weaver R, Webborn P. 2003. Hit-to-Lead studies: The discovery of potent adamantane amide P2X7 receptor antagonists. Bioorg. Med. Chem. Lett. 13:4047–4050.

88. Beaulieu PL, Bös M, Bousquet Y, Fazal G, Gauthier J, Gillard J, Goulet S, LaPlante S, Poupart M-A, Lefebvre S, McKercher G, Pellerin C, Austel V, Kukolj G. 2004. Non-nucleoside inhibitors of the hepatitis C virus NS5B polymerase: discovery and preliminary SAR of benzimidazole derivatives. Bioorg. Med. Chem. Lett. 14:119–124.

89. Langdon SR, Ertl P, Brown N. 2010. Bioisosteric replacement and scaffold hopping in lead generation and optimization. Mol. Inform. 29:366–385.

90. Blaser A, Palmer BD, Sutherland HS, Kmentova I, Franzblau SG, Wan B, Wang Y, Ma Z, Thompson AM, Denny WA. 2012. Structure–activity relationships for amide-, carbamate-, and urea-linked analogues of the tuberculosis drug (6S)-2-nitro-6-{[4-(trifluoromethoxy)benzyl]oxy}-6,7-dihydro-5H-imidazo[2,1-b][1,3]oxazine (PA-824). J. Med. Chem. 55:312–326.

91. Annis DA, Nazef N, Chuang C-C, Scott MP, Nash HM. 2004. A general technique to rank protein−ligand binding affinities and determine allosteric versus direct binding site competition in compound mixtures. J. Am. Chem. Soc. 126:15495–15503.

92. Reynolds CH, Bembenek SD, Tounge BA. 2007. The role of molecular size in ligand efficiency. Bioorg. Med. Chem. Lett. 17:4258–4261.

93. Dahan A, Miller JM. 2012. The solubility–permeability interplay and its implications in formulation design and development for poorly soluble drugs. AAPS J. 14:244–251.

94. Mortelmans K, Zeiger E. 2000. The Ames Salmonella/microsome mutagenicity assay. Mutat. Res. Mol. Mech. Mutagen. 455:29–60.

95. Roux S, Sablé E, Porsolt RD. 2005. Primary observation (Irwin) test in rodents for assessing acute toxicity of a test agent and its effects on behavior and physiological function, p. *In* Enna, SJ, Williams, M, Barret, JF, Ferkany, JW, Kenakin, T, Porsolt,

RD (eds.), Current Protocols in Pharmacology. John Wiley & Sons, Inc., Hoboken, NJ, USA.

96. Lienhardt C, Vernon A, Raviglione MC. 2010. New drugs and new regimens for the treatment of tuberculosis: review of the drug development pipeline and implications for national programmes. Curr. Opin. Pulm. Med. 16:186–193.
97. Streiner DL, Norman GR. 2009. Drug Trial Phases. Community Oncol. 6:37–40.
98. Sarathy J, Dartois V, Dick T, Gengenbacher M. 2013. Reduced drug uptake in phenotypically resistant nutrient-starved nonreplicating *Mycobacterium tuberculosis*. Antimicrob. Agents Chemother. 57:1648–1653.
99. Hugonnet J-E, Tremblay LW, Boshoff HI, Barry CE, Blanchard JS. 2009. Meropenem-clavulanate is effective against extensively drug-resistant *Mycobacterium tuberculosis*. Science 323:1215–1218.
100. Cholo MC, Steel HC, Fourie PB, Germishuizen WA, Anderson R. 2011. Clofazimine: current status and future prospects. J. Antimicrob. Chemother.
101. Van Rensburg CEJ, Anderson R, O'Sullivan JF. 1997. Riminophenazine compounds: pharmacology and anti-neoplastic potential. Crit. Rev. Oncol. Hematol. 25:55–67.
102. Lienhardt C, Vernon A, Raviglione MC. 2010. New drugs and new regimens for the treatment of tuberculosis: review of the drug development pipeline and implications for national programmes. Curr. Opin. Pulm. Med. 1.
103. Ma Z, Lienhardt C, McIlleron H, Nunn AJ, Wang X. 2010. Global tuberculosis drug development pipeline: the need and the reality. The Lancet 375:2100–2109.
104. Zumla AI, Gillespie SH, Hoelscher M, Philips PPJ, Cole ST, Abubakar I, McHugh TD, Schito M, Maeurer M, Nunn AJ. 2014. New antituberculosis drugs, regimens, and adjunct therapies: needs, advances, and future prospects. Lancet Infect. Dis. 14:327–340.
105. Cole ST, Riccardi G. 2011. New tuberculosis drugs on the horizon. Curr. Opin. Microbiol. 14:570–576.
106. Evaluation of Early Bactericidal Activity in Pulmonary Tuberculosis With Clofazimine (C)-TMC207 (J)-PA-824 (Pa)-Pyrazinamide (Z) (NC-003). Global Alliance of TB Drug Development.
107. Andries K, Villellas C, Coeck N, Thys K, Gevers T, Vranckx L, Lounis N, de Jong BC, Koul A. 2014. Acquired resistance of *Mycobacterium tuberculosis* to bedaquiline. PLoS ONE 9.

108. Hartkoorn RC, Upekar S, Cole ST. 2014. Cross-resistance between clofazimine and bedaquiline through up-regulation of MmpL5 in *Mycobacterium tuberculosis*. Antimicrob. Agents Chemother. AAC.00037–14.
109. Somoskovi A, Bruderer V, Hömke R, Bloemberg GV, Böttger EC. 2014. A mutation associated with clofazimine and bedaquiline cross-resistance in MDR-TB following bedaquiline treatment. Eur. Respir. J. erj01429–2014.
110. Lienhardt C, Raviglione M, Spigelman M, Hafner R, Jaramillo E, Hoelscher M, Zumla A, Gheuens J. 2012. New Drugs for the treatment of tuberculosis: needs, challenges, promise, and prospects for the future. J. Infect. Dis. 205:S241–S249.
111. Donald PR, Diacon AH. 2008. The early bactericidal activity of anti-tuberculosis drugs: a literature review. Tuberc. Edinb. Scotl. 88 Suppl 1:S75–83.
112. Diacon AH, Dawson R, Bois J du, Narunsky K, Venter A, Donald PR, Niekerk C van, Erondu N, Ginsberg AM, Becker P, Spigelman MK. 2012. Phase II dose-ranging trial of the early bactericidal activity of PA-824. Antimicrob. Agents Chemother. 56:3027–3031.
113. Gumbo T, Drusano GL, Liu W, Ma L, Deziel MR, Drusano MF, Louie A. 2006. Anidulafungin pharmacokinetics and microbial response in neutropenic mice with disseminated candidiasis. Antimicrob. Agents Chemother. 50:3695–3700.
114. Diacon AH, Dawson R, von Groote-Bidlingmaier F, Symons G, Venter A, Donald PR, van Niekerk C, Everitt D, Winter H, Becker P, Mendel CM, Spigelman MK. 2012. 14-Day bactericidal activity of PA-824, bedaquiline, pyrazinamide, and moxifloxacin combinations: a randomised trial. Lancet 380:986–993.
115. Mahajan R. 2013. Bedaquiline: first FDA-approved tuberculosis drug in 40 years. Int. J. Appl. Basic Med. Res. 3:1–2.
116. Diacon AH, Pym A, Grobusch M, Patientia R, Rustomjee R, Page-Shipp L, Pistorius C, Krause R, Bogoshi M, Churchyard G, Venter A, Allen J, Palomino JC, De Marez T, van Heeswijk RPG, Lounis N, Meyvisch P, Verbeeck J, Parys W, de Beule K, Andries K, Neeley DFM. 2009. The diarylquinoline TMC207 for multidrug-resistant tuberculosis. N. Engl. J. Med. 360:2397–2405.
117. Huitric E, Verhasselt P, Andries K, Hoffner SE. 2007. *in vitro* antimycobacterial spectrum of a diarylquinoline ATP synthase inhibitor. Antimicrob. Agents Chemother. 51:4202–4204.
118. Kamerbeek J, Schouls L, Kolk A, van Agterveld M, van Soolingen D, Kuijper S, Bunschoten A, Molhuizen H, Shaw R, Goyal M, van Embden J. 1997. Simultaneous

detection and strain differentiation of *Mycobacterium tuberculosis* for diagnosis and epidemiology. J. Clin. Microbiol. 35:907–914.

119. Cole ST, Brosch R, Parkhill J, Garnier T, Churcher C, Harris D, Gordon SV, Eiglmeier K, Gas S, Barry CE, Tekaia F, Badcock K, Basham D, Brown D, Chillingworth T, Connor R, Davies R, Devlin K, Feltwell T, Gentles S, Hamlin N, Holroyd S, Hornsby T, Jagels K, Krogh A, McLean J, Moule S, Murphy L, Oliver K, Osborne J, Quail MA, Rajandream M-A, Rogers J, Rutter S, Seeger K, Skelton J, Squares R, Squares S, Sulston JE, Taylor K, Whitehead S, Barrell BG. 1998. Deciphering the biology of *Mycobacterium tuberculosis* from the complete genome sequence. Nature 393:537–544.
120. Bolger AM, Lohse M, Usadel B. 2014. Trimmomatic: A flexible trimmer for Illumina sequence data. Bioinformatics btu170.
121. Li H, Durbin R. 2009. Fast and accurate short read alignment with Burrows-Wheeler transform. Bioinforma. Oxf. Engl. 25:1754–1760.
122. McKenna A, Hanna M, Banks E, Sivachenko A, Cibulskis K, Kernytsky A, Garimella K, Altshuler D, Gabriel S, Daly M, DePristo MA. 2010. The Genome Analysis Toolkit: A MapReduce framework for analyzing next-generation DNA sequencing data. Genome Res. 20:1297–1303.
123. Hall TA. 1999. BioEdit: a user-friendly biological sequence alignment editor and analysis program for Windows 95/98/NT. Nucleic Acids Symp Ser 41:95–98.
124. Radhakrishnan A, Kumar N, Wright CC, Chou T-H, Tringides ML, Bolla JR, Lei H-T, Rajashankar K, Su C-C, Purdy GE, Yu EW. 2014. Crystal structure of the transcriptional regulator Rv0678 of *Mycobacterium tuberculosis*. J. Biol. Chem. jbc.M113.538959.
125. Arnold K, Bordoli L, Kopp J, Schwede T. 2006. The SWISS-MODEL workspace: a web-based environment for protein structure homology modelling. Bioinforma. Oxf. Engl. 22:195–201.
126. Biasini M, Bienert S, Waterhouse A, Arnold K, Studer G, Schmidt T, Kiefer F, Cassarino TG, Bertoni M, Bordoli L, Schwede T. 2014. SWISS-MODEL: modelling protein tertiary and quaternary structure using evolutionary information. Nucleic Acids Res. 42:W252–258.
127. Bordoli L, Kiefer F, Arnold K, Benkert P, Battey J, Schwede T. 2008. Protein structure homology modeling using SWISS-MODEL workspace. Nat. Protoc. 4:1–13.

128. Pettersen EF, Goddard TD, Huang CC, Couch GS, Greenblatt DM, Meng EC, Ferrin TE. 2004. UCSF Chimera--a visualization system for exploratory research and analysis. J. Comput. Chem. 25:1605–1612.
129. Lebreton F, van Schaik W, Sanguinetti M, Posteraro B, Torelli R, Le Bras F, Verneuil N, Zhang X, Giard J-C, Dhalluin A, Willems RJL, Leclercq R, Cattoir V. 2012. AsrR is an oxidative stress sensing regulator modulating *Enterococcus faecium* opportunistic traits, antimicrobial resistance, and pathogenicity. PLoS Pathog. 8:e1002834.
130. Milano A, Pasca MR, Provvedi R, Lucarelli AP, Manina G, Luisa de Jesus Lopes Ribeiro A, Manganelli R, Riccardi G. 2009. Azole resistance in *Mycobacterium tuberculosis* is mediated by the MmpS5–MmpL5 efflux system. Tuberculosis 89:84–90.
131. Wells RM, Jones CM, Xi Z, Speer A, Danilchanka O, Doornbos KS, Sun P, Wu F, Tian C, Niederweis M. 2013. Discovery of a siderophore export system essential for virulence of *Mycobacterium tuberculosis*. PLoS Pathog. 9.
132. Wilkinson SP, Grove A. 2006. Ligand-responsive transcriptional regulation by members of the MarR family of winged helix proteins. Curr. Issues Mol. Biol. 8:51–62.
133. Wilkinson SP, Grove A. 2004. HucR, a novel uric acid-responsive member of the MarR family of transcriptional regulators from *Deinococcus radiodurans*. J. Biol. Chem. 279:51442–51450.
134. Varela C, Rittmann D, Singh A, Krumbach K, Bhatt K, Eggeling L, Besra GS, Bhatt A. 2012. MmpL genes are associated with mycolic acid metabolism in mycobacteria and corynebacteria. Chem. Biol. 19:498–506.
135. Domenech P, Reed MB, Barry CE. 2005. Contribution of the *Mycobacterium tuberculosis* MmpL protein family to virulence and drug resistance. Infect. Immun. 73:3492–3501.
136. Jain M, Cox JS. 2005. Interaction between polyketide synthase and transporter suggests coupled synthesis and export of virulence lipid in *M. tuberculosis*. PLoS Pathog 1:e2.
137. Cox JS, Chen B, McNeil M, Jacobs WR. 1999. Complex lipid determines tissue-specific replication of *Mycobacterium tuberculosis* in mice. Nature 402:79–83.
138. Converse SE, Mougous JD, Leavell MD, Leary JA, Bertozzi CR, Cox JS. 2003. MmpL8 is required for sulfolipid-1 biosynthesis and *Mycobacterium tuberculosis* virulence. Proc. Natl. Acad. Sci. U. S. A. 100:6121–6126.

139. Pacheco SA, Hsu F-F, Powers KM, Purdy GE. 2013. MmpL11 protein transports mycolic acid-containing lipids to the mycobacterial cell wall and contributes to biofilm formation in *Mycobacterium smegmatis*. J. Biol. Chem. 288:24213–24222.
140. Ratledge C. 2004. Iron, mycobacteria and tuberculosis. Tuberculosis 84:110–130.
141. Bacon J, Dover LG, Hatch KA, Zhang Y, Gomes JM, Kendall S, Wernisch L, Stoker NG, Butcher PD, Besra GS, Marsh PD. 2007. Lipid composition and transcriptional response of *Mycobacterium tuberculosis* grown under iron-limitation in continuous culture: identification of a novel wax ester. Microbiol. Read. Engl. 153:1435–1444.
142. Weinstein EA, Yano T, Li L-S, Avarbock D, Avarbock A, Helm D, McColm AA, Duncan K, Lonsdale JT, Rubin H. 2005. Inhibitors of type II NADH:menaquinone oxidoreductase represent a class of antitubercular drugs. Proc. Natl. Acad. Sci. U. S. A. 102:4548–4553.
143. Nakamaru-Ogiso E, Yano T, Ohnishi T, Yagi T. 2002. Characterization of the iron-sulfur cluster coordinated by a cysteine cluster motif (CXXCXXXCX 27C) in the Nqo3 subunit in the proton-translocating NADH-quinone oxidoreductase (NDH-1) of *Thermus thermophilus* HB-8. J. Biol. Chem. 277:1680–1688.
144. Pasca MR, Guglierame P, Rossi ED, Zara F, Riccardi G. 2005. *mmpL7* gene of *Mycobacterium tuberculosis* is responsible for isoniazid efflux in *Mycobacterium smegmatis*. Antimicrob. Agents Chemother. 49:4775–4777.
145. Wells RM. 2012. Siderophore-mediated iron acquisition in *Mycobacterium tuberculosis*. The University of Alabama at Birmingham.
146. Voss JJD, Rutter K, Schroeder BG, Barry CE. 1999. Iron acquisition and metabolism by mycobacteria. J. Bacteriol. 181:4443–4451.
147. Fitzmaurice AM, Kolattukudy PE. 1997. Open reading frame 3, which is adjacent to the mycocerosic acid synthase gene, is expressed as an acyl coenzyme A synthase in *Mycobacterium bovis* BCG. J. Bacteriol. 179:2608–2615.
148. Sirakova TD, Fitzmaurice AM, Kolattukudy P. 2002. Regulation of expression of *mas* and *fadD28*, two genes involved in production of dimycocerosyl phthiocerol, a virulence factor of *Mycobacterium tuberculosis*. J. Bacteriol. 184:6796–6802.
149. Bisson GP, Mehaffy C, Broeckling C, Prenni J, Rifat D, Lun DS, Burgos M, Weissman D, Karakousis PC, Dobos K. 2012. Upregulation of the phthiocerol dimycocerosate biosynthetic pathway by rifampin-resistant, *rpoB* mutant *Mycobacterium tuberculosis*. J. Bacteriol. 194:6441–6452.

150. Camacho LR, Constant P, Raynaud C, Lanéelle M-A, Triccas JA, Gicquel B, Daffé M, Guilhot C. 2001. Analysis of the phthiocerol dimycocerosate locus of *Mycobacterium tuberculosis* evidence that this lipid is involved in the cell wall permeability barrier. J. Biol. Chem. 276:19845–19854.

151. Domenech P, Reed MB. 2009. Rapid and spontaneous loss of phthiocerol dimycocerosate (PDIM) from *Mycobacterium tuberculosis* grown in vitro: implications for virulence studies. Microbiology 155:3532–3543.

152. Goren MB, Brokl O, Schaefer WB. 1974. Lipids of putative relevance to virulence in *Mycobacterium tuberculosis*: phthiocerol dimycocerosate and the attenuation indicator lipid. Infect. Immun. 9:150–158.

153. Titgemeyer F, Amon J, Parche S, Mahfoud M, Bail J, Schlicht M, Rehm N, Hillmann D, Stephan J, Walter B, Burkovski A, Niederweis M. 2007. A genomic view of sugar transport in *Mycobacterium smegmatis* and *Mycobacterium tuberculosis*. J. Bacteriol. 189:5903–5915.

154. Jamshidi N, Palsson BØ. 2007. Investigating the metabolic capabilities of *Mycobacterium tuberculosis* H37Rv using the *in silico* strain iNJ661 and proposing alternative drug targets. BMC Syst. Biol. 1:26.

155. Sassetti CM, Boyd DH, Rubin EJ. 2003. Genes required for mycobacterial growth defined by high density mutagenesis. Mol. Microbiol. 48:77–84.

156. Keating LA, Wheeler PR, Mansoor H, Inwald JK, Dale J, Hewinson RG, Gordon SV. 2005. The pyruvate requirement of some members of the *Mycobacterium tuberculosis* complex is due to an inactive pyruvate kinase: implications for *in vivo* growth. Mol. Microbiol. 56:163–174.

157. Franceschini A, Szklarczyk D, Frankild S, Kuhn M, Simonovic M, Roth A, Lin J, Minguez P, Bork P, von Mering C, Jensen LJ. 2013. STRING v9.1: protein-protein interaction networks, with increased coverage and integration. Nucleic Acids Res. 41:D808–815.

158. Jensen LJ, Kuhn M, Stark M, Chaffron S, Creevey C, Muller J, Doerks T, Julien P, Roth A, Simonovic M, Bork P, von Mering C. 2009. STRING 8 - a global view on proteins and their functional interactions in 630 organisms. Nucleic Acids Res. 37:D412–416.

159. Snel B, Lehmann G, Bork P, Huynen MA. 2000. STRING: a web-server to retrieve and display the repeatedly occurring neighbourhood of a gene. Nucleic Acids Res. 28:3442–3444.

160. Szklarczyk D, Franceschini A, Kuhn M, Simonovic M, Roth A, Minguez P, Doerks T, Stark M, Muller J, Bork P, Jensen LJ, von Mering C. 2011. The STRING database in 2011: functional interaction networks of proteins, globally integrated and scored. Nucleic Acids Res. 39:D561–568.
161. Von Mering C, Jensen LJ, Kuhn M, Chaffron S, Doerks T, Krüger B, Snel B, Bork P. 2007. STRING 7- recent developments in the integration and prediction of protein interactions. Nucleic Acids Res. 35:D358–362.
162. Von Mering C, Jensen LJ, Snel B, Hooper SD, Krupp M, Foglierini M, Jouffre N, Huynen MA, Bork P. 2005. STRING: known and predicted protein-protein associations, integrated and transferred across organisms. Nucleic Acids Res. 33:D433–437.
163. Von Mering C, Huynen M, Jaeggi D, Schmidt S, Bork P, Snel B. 2003. STRING: a database of predicted functional associations between proteins. Nucleic Acids Res. 31:258–261.

Addendum

BACTEC™ MGIT™ 960 Drug Concentration Equations

$$\frac{(\text{Final Drug Concentration in MGIT Tube}) \times (\text{MGIT Tube Volume})}{(\text{Drug Stock Concentration})} \times 1\,000 = x \text{ ml}$$

$$\frac{(\text{Drug Stock Concentration})}{(\text{Volume Used to Inoculate MGIT Tube})} \times x \text{ ml} = y \text{ µg/ml}$$

$$\frac{(y \text{ µg/ml}) \times (\text{Volume of } ddH_2O^* \text{ Used To Dilute Drug})}{(\text{Drug Stock Concentration})} = z \text{ ml}$$

*ddH_2O : double distilled water

MGIT Tube Volume: 8.4 ml

Volume Used to Inoculate MGIT Tube: 100 µl

Volume of ddH_2O Used to Dilute Drug: 1 ml

The final drug concentration is obtained when *z* ml is diluted with ddH_2O to a final volume of 1 ml.